water

MDPI

Article

Extreme-Rainfall Estimate and Return Levels in the Niger Delta Basin: A Comparative Analysis of Probability Distribution Models

Oye Ideki [1,*], Anthony R. Lupo [2], Temi Emmanuel Ologunorisa [3], Charles Ichoku [4] and Omolola Akinola Ologunorisa [5]

[1] Department of History and Geography, Morgan State University, Baltimore, MD 21251, USA;
[2] Atmospheric Sciences Program, School of Natural Resources, University of Missouri, Columbia, MO 65211, USA; lupoa@missouri.edu
[3] Department of Meteorology and Climate Change, Federal University of Technology, Akure 340001, Nigeria
[4] Department of Geography and Environmental Systems and Goddard Earth Sciences Technology and Research (GESTAR II), University of Maryland, Baltimore County (UMBC), Baltimore, MD 21250, USA; cichoku@umbc.edu
[5] Department of Political Science and Geography, Old Dominion University, Norfolk, VA 23529, USA; oologuno@odu.edu
* Correspondence: oye.ideki@morgan.edu

Abstract

Accurate estimation of extreme rainfall is essential for flood-risk assessment, hydrological planning, and climate adaptation in the Niger Delta, Nigeria. This study investigated rainfall variability, extreme precipitation characteristics, and rainfall return levels across Bayelsa, Rivers, and Delta States using Climate Hazards Group InfraRed Precipitation with Station Data (CHIRPS) observations for 1983–2023. The analysis incorporated descriptive statistics, rainfall trend and change-point tests, annual block maxima, Gumbel and Log-Pearson Type III (LP3) distributions, Peaks-Over-Threshold analysis using the Generalized Pareto Distribution (POT-GPD), Bayesian Gumbel inference, and stationary and non-stationary Generalized Extreme Value (GEV) sensitivity analysis. Each state contained 14,975 daily rainfall observations and 41 annual maximum daily (AMAX-D) and annual maximum monthly (AMAX-M) values. Bayelsa recorded the highest mean annual rainfall (3109.47 mm), followed by Rivers (2766.92 mm) and Delta (2393.78 mm). The highest observed daily rainfall was 126.73 mm in Rivers, 125.37 mm in Bayelsa, and 93.72 mm in Delta. Daily rainfall distributions exhibited positive skewness, with coefficients ranging from 2.25 to 2.42, indicating pronounced upper-tail variability. Annual rainfall totals showed substantial interannual fluctuations without statistically significant linear trends ($p > 0.05$). For AMAX-D, the Gumbel distribution recorded lower Akaike Information Criterion (AIC) and Bayesian Information Criterion (BIC) values across all three states, although LP3 achieved lower quantile–quantile root mean square errors in Bayelsa and Rivers. For AMAX-M, LP3 achieved lower AIC values and quantile–quantile errors across all three states, while BIC favoured Gumbel in Rivers and Delta. The estimated 100-year Gumbel daily rainfall return levels were 136.71 mm, 121.41 mm, and 103.26 mm for Bayelsa, Rivers, and Delta, respectively. Corresponding monthly return levels were 910.92 mm, 760.52 mm, and 684.28 mm. The POT-GPD analysis produced 100-year daily return levels of 134.70 mm, 124.21 mm, and 96.99 mm, respectively. The stationary GEV specification recorded lower BIC values across all six state-specific comparisons, while the non-stationary model achieved a marginally lower AIC for Delta monthly maxima without statistically significant improvement. The

Academic Editor: Ataur Rahman

Received: 18 September 2026
Revised: 15 November 2026
Accepted: 20 November 2026
Published: 24 November 2026

Copyright: © 2026 by the authors. Licensee MDPI, Basel, Switzerland. This article is an open access article distributed under the terms and conditions of the Creative Commons Attribution (CC BY) license.

findings demonstrate substantial spatial differences in rainfall magnitude, pronounced upper-tail variability, and sensitivity of estimated extreme-rainfall return levels to probability distribution selection and accumulation period. The results support state-specific flood hazard assessment and emphasize the importance of parameter uncertainty, model selection, and careful interpretation of extrapolated return levels in flood-risk management, infrastructure planning, and climate adaptation.

Keywords: CHIRPS; extreme rainfall; Niger Delta; rainfall variability; Gumbel distribution; Log-Pearson Type III; POT-GPD; generalized extreme value; return levels; climate adaptation

1. Introduction

Extreme rainfall is a key climatic variable with significant implications for hydrological processes, ecological systems, river dynamics, infrastructure, and human livelihoods. These impacts are particularly important in the Niger Delta Basin, where rainfall interacts with low-lying terrain, extensive river and creek networks, tidal processes, and adjacent land–water dynamics [1–3]. Recent studies indicate that climate variability and climate change are altering the frequency, intensity, timing, and spatial distribution of heavy rainfall at regional and global scales [4–6]. Observed and projected changes in rainfall characteristics can modify streamflow regimes, increase flood exposure, disrupt livelihoods, damage infrastructure, and complicate water-resource management [7,8]. Consequently, understanding the characteristics and probabilities of extreme rainfall is important for flood-risk assessment, climate adaptation, and the planning of resilient infrastructure in the Niger Delta [9].

According to the World Meteorological Organization [10], extreme rainfall is more appropriately defined using statistical criteria than by assigning it a fixed recurrence interval [11]. Depending on the analytical framework, an extreme event may be represented by an annual maximum, a high rainfall percentile, or an observation exceeding a specified threshold [12]. In frequency analysis, the rarity of an event is commonly expressed through its return period. For example, under a stationary model, a rainfall magnitude associated with a 100-year return period has an annual exceedance probability of approximately 1% [13]. This does not mean that the event occurs regularly once every 100 years; rather, it represents the probability that the specified rainfall magnitude will be exceeded in any given year. This distinction is important for the interpretation and communication of extreme-rainfall risk [14].

Extreme rainfall is an important contributor to flooding in many regions, and the Niger Delta is particularly vulnerable because of its deltaic terrain, high rainfall regime, extensive network of rivers and creeks, coastal influences, rapid urban development, and drainage limitations [15,16]. Historical flood events illustrate the severity of the problem. The 2012 Nigerian flood disaster resulted in hundreds of fatalities, displaced millions of people, and caused substantial economic losses [17]. Major flooding was again recorded in subsequent years, affecting several states, including Delta, Bayelsa, Rivers, Edo, Anambra, Kogi, and Benue [18–20]. Such events demonstrate the continuing importance of reliable hydrometeorological risk assessment in Nigeria.

However, extreme rainfall should not be considered synonymous with flooding. Flood magnitude depends on several interacting factors, including rainfall intensity and duration, antecedent soil moisture, catchment characteristics, river discharge, drainage capacity, topography, land-use change, and, in coastal environments, tidal and sea-level conditions. Rainfall-frequency analysis therefore represents one component of

comprehensive flood-risk assessment. Extreme-rainfall-frequency analysis has long been used in hydrology and climate science to characterize the statistical properties of rare precipitation events and estimate rainfall magnitudes associated with specified probabilities or return periods [21]. Extreme Value Theory (EVT) provides a theoretical foundation for characterizing rare rainfall events and estimating return levels. Statistical approaches, including Bayesian inference and Peaks-Over-Threshold (POT) analysis, together with probability distributions such as Gumbel and Log-Pearson Type III, offer complementary methods for estimating extreme-rainfall magnitudes and quantifying associated uncertainties.

Bayesian inference combines a specified likelihood with prior distributions to estimate posterior parameter distributions. Propagating posterior draws through the return-level equation quantifies parameter uncertainty, conditional on the selected model and prior assumptions. Posterior convergence alone does not establish predictive accuracy.

The Peaks-Over-Threshold (POT) approach uses observations exceeding a sufficiently high threshold rather than selecting only one maximum observation from each year, thereby allowing a larger sample of extreme-rainfall events to be considered in frequency analysis.

The POT/GPD approach has an important advantage over annual block maxima because it can retain multiple sufficiently extreme observations within a year, thereby making greater use of information contained in the upper tail. However, reliable application requires careful threshold selection and consideration of the independence of successive exceedances. In addition to the statistical frequency analyses discussed above, numerical atmospheric models provide an important framework for investigating extreme precipitation [22]. Recent studies in Nigeria and West Africa have demonstrated the application of regional climate models and high-resolution simulations in assessing rainfall extremes and potential future changes [23–25]. Higher-resolution models can improve the representation of localized heavy rainfall, although their performance depends on spatial resolution, physical parameterizations, and boundary conditions [26]. Numerical modelling and statistical extreme-value analysis therefore provide complementary approaches: the former examines atmospheric processes and potential future changes, while the latter estimates the frequency and magnitude of rainfall extremes from historical records [27]. The present study adopts statistical extreme-value analysis using CHIRPS rainfall data to characterize rainfall extremes and return levels in the Niger Delta region of Nigeria.

Various probability distributions have previously been applied to rainfall-frequency analysis in Nigeria and the Niger Delta. Reference [28] applied Gumbel, Pearson Type III, and Log-Pearson Type III distributions to rainfall-frequency and return-period analyses. Studies [5,29] examined probability distributions for rainfall return-period estimation at locations within the Niger Delta and reported differences in model performance among candidate distributions. Earlier studies [30–32] investigated rainfall variability, urban flooding, and related hydrological characteristics, while [33] examined rainfall intensity–duration–frequency relationships in Lagos. These studies demonstrate the usefulness of statistical distributions for rainfall-frequency analysis but also indicate that model performance depends on location, sample characteristics, temporal aggregation, and upper-tail behaviour.

Although previous investigations have used extreme-value distributions for rainfall analysis in southern Nigeria, direct comparisons across temporal aggregation scales and alternative tail models remain useful. The contribution of this study is the integration of Bayesian Gumbel inference, classical Gumbel and Log-Pearson Type III distributions, declustered Peaks-Over-Threshold analysis using the Generalized Pareto Distribution,

and non-stationary Generalized Extreme Value modelling. The study further distinguishes annual maximum daily rainfall from annual maximum monthly rainfall, quantifying parameter and return-level uncertainty, evaluating distributional goodness of fit, and examining the implications of potential non-stationarity. Rather than proposing a new statistical distribution, the study provides a comparative assessment of established statistical methods within a common regional framework, offering insights into the sensitivity of extreme-rainfall estimates and whether a time-varying GEV location parameter improves fit.

Arising from above, the study objectives are to (i) define and validate the rainfall series and their spatial aggregation, (ii) estimate annual rainfall trends and variability using linear regression, (iii) compare Gumbel and Log-Pearson Type III fits to annual daily and monthly maxima, (iv) quantify Bayesian Gumbel parameter and return-level uncertainty, (v) evaluate POT/GPD fits using threshold and declustering sensitivity analyses, and (vi) assess change points and stationary versus non-stationary GEV fits with uncertainty-aware model diagnostics.

2. Materials and Methods

2.1. Study Area

The Niger Delta is one of the largest deltas in the world, covering over 20,000 km^2 in southern Nigeria [34]. In terms of the hydrogeological setting, the coastal Niger Delta is dominated by an extensive wetland formed by the increase in sedimentary materials drained by the Niger and Benue Rivers [35]. Although extreme rainfall is an important contributor to flooding, flood occurrence in the Niger Delta also depends on river discharge, antecedent soil moisture, drainage conditions, tidal processes, land-use change, and other catchment characteristics. Climatically, the Niger Delta has a humid tropical climate typical of the coastal zone of West Africa. Seasonal rainfall variability is strongly influenced by the West African monsoon system and the seasonal migration of the tropical rain belt, commonly associated with the Intertropical Convergence Zone (ITCZ). These atmospheric circulation processes contribute to the prolonged wet season experienced across much of the region, generally extending from approximately March to October, although the timing and magnitude of rainfall vary spatially and interannually [36]. Annual rainfall is generally high, with some parts of the coastal Niger Delta receiving approximately 3000 mm or more per year, while mean annual temperatures are around 28 °C, although both rainfall and temperature vary spatially across the region. The annual rainfall cycle may exhibit two rainfall peaks in parts of southern Nigeria, reflecting seasonal changes in the monsoon circulation and migration of the tropical rain belt. These climatic characteristics provide favourable conditions for high rainfall totals and episodic extreme-rainfall events.

The three states included in the study—Rivers, Bayelsa, and Delta—also contain substantial populations and important urban, agricultural, industrial, and petroleum-producing areas. According to the source cited in [37], the estimated populations of the three states are 8,003,818, 2,725,159, and 6,010,334, respectively, representing a combined population of approximately 16.74 million inhabitants.

Population growth, urban expansion, infrastructure development, and modifications to natural drainage systems in the Niger Delta have increased exposure and vulnerability to rainfall-related flooding [38]. The region is characterized by an extensive network of distributary rivers, creeks, channels, and wetlands, with the lower River Niger dividing into major distributaries, including the Forcados and Nun Rivers, before discharging into the Gulf of Guinea [39]. The proximity of settlements and economic activities to these waterways increases exposure to the combined effects of extreme rainfall, river flooding, and coastal processes [40]. For this study, Rivers, Bayelsa, and Delta States constitute the

defined spatial domain for the 1983–2023 extreme-rainfall analysis. The combination of high rainfall, low-lying terrain, dense drainage networks, extensive wetlands, coastal influences, and human settlement makes the region particularly suitable for evaluating rainfall variability and extreme-rainfall frequency [38,40].

The geographical extent and location of the three-state study area is presented in Figure 1.

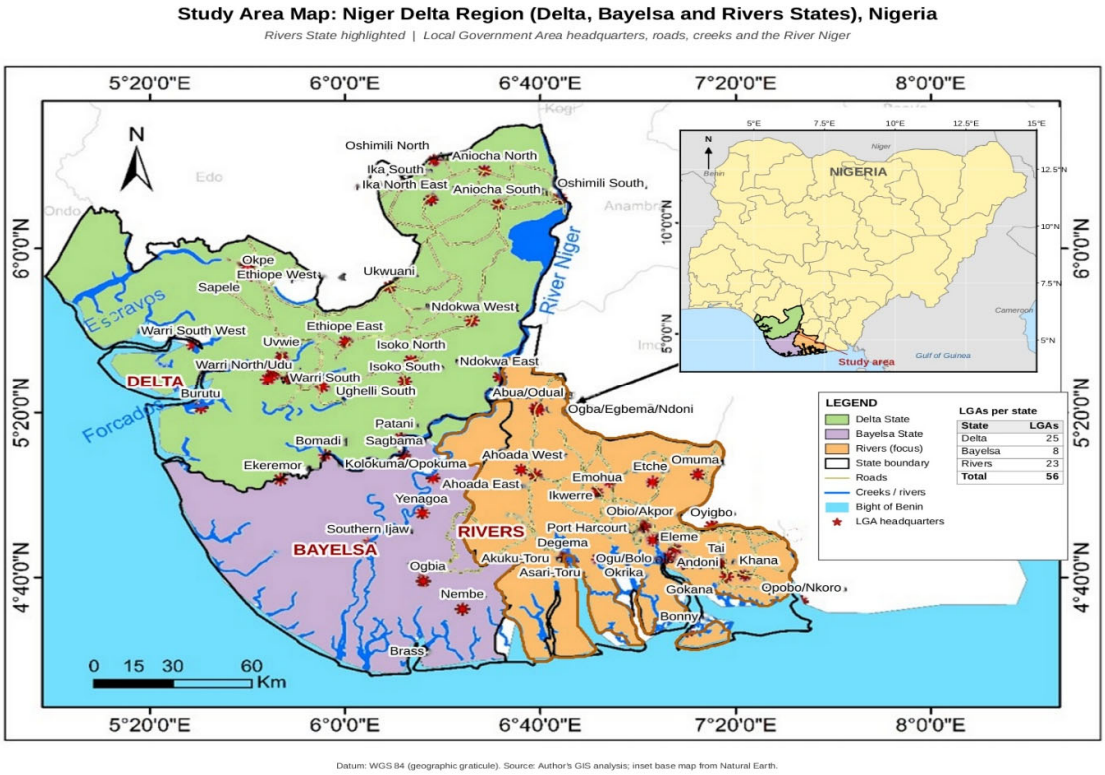


Figure 1. Map of the study area showing the coastal Niger Delta region.

2.2. Rainfall Data and Analytical Methods

Daily rainfall data for the period 1983–2023 were obtained from the Climate Hazards Group InfraRed Precipitation with Station Data (CHIRPS), developed by the Climate Hazards Center at the University of California, Santa Barbara. CHIRPS integrates satellite-derived infrared precipitation estimates with ground-based rainfall observations to provide long-term precipitation records at approximately 0.05° spatial resolution [41]. Rainfall data covering Rivers, Bayelsa, and Delta States were extracted to characterize rainfall variability and extreme precipitation in the Niger Delta region. State-level daily rainfall estimates were used to derive monthly and annual rainfall totals for subsequent statistical analyses. Data quality and temporal consistency were assessed through checks for missing observations, duplicate records, anomalous values, and inconsistencies across temporal aggregations. The various methods used in the analysis is summarized in Figure 2. The resulting rainfall series provided the basis for the statistical frequency analysis and estimation of extreme-rainfall return levels.

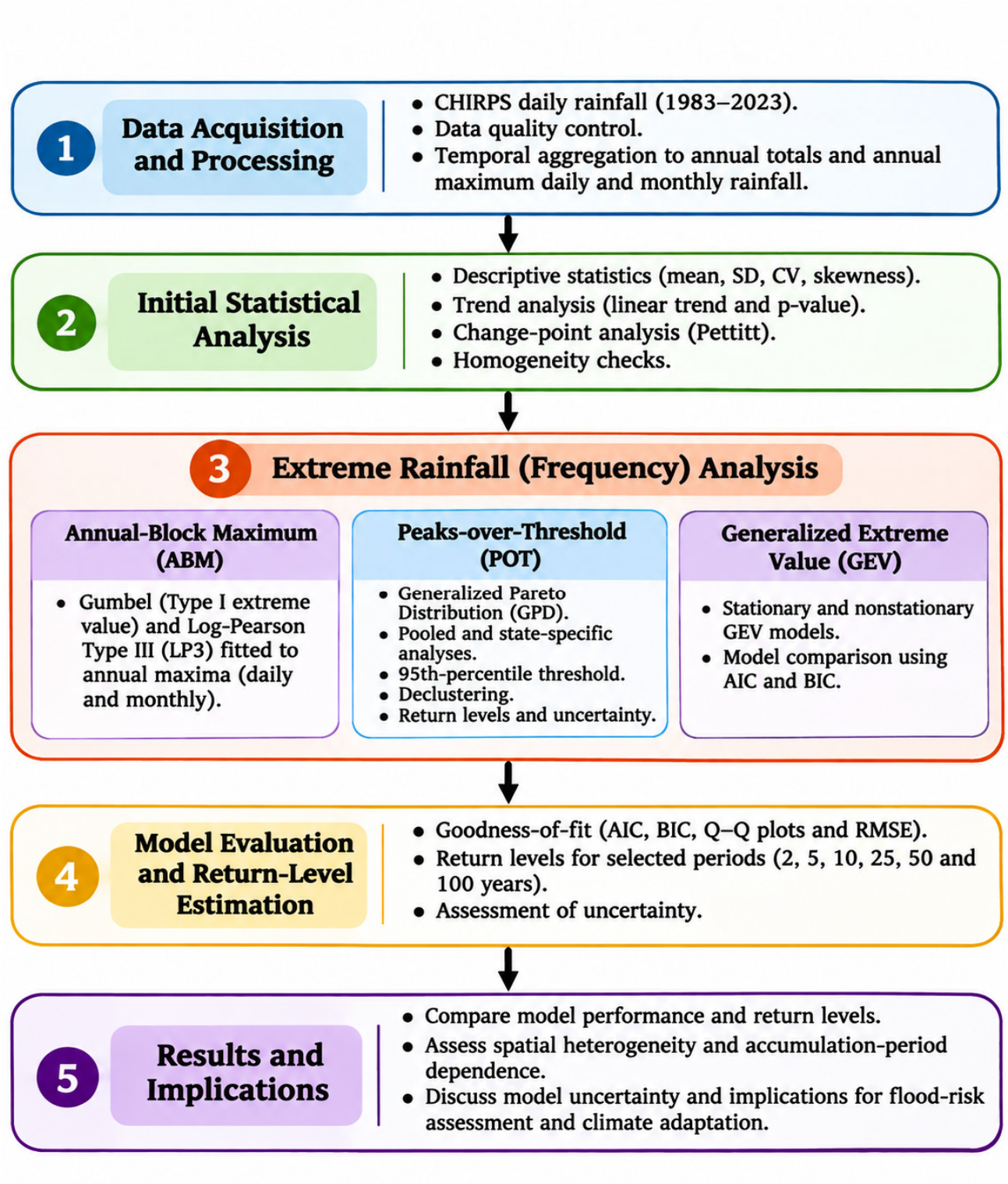


Figure 2. Detailed flowchart of the adopted methods.

2.2.1. Rainfall Data and Temporal Aggregation

Daily precipitation data for Bayelsa, Rivers, and Delta States were obtained from the Climate Hazards Group InfraRed Precipitation with Station Data (CHIRPS) for the period 1 January 1983 to 31 December 2023. The dataset provides satellite-derived precipitation estimates incorporating ground-based rainfall observations at approximately 0.05° spatial

resolution. Daily rainfall estimates were spatially aggregated to represent each state, providing consistent time series for evaluating rainfall variability, annual precipitation characteristics, and extreme-rainfall events.

The analysis covered 41 consecutive years, comprising 14,975 daily observations per state and 44,925 state-day observations across the three states. The dataset included ten leap years, each containing 366 days. Monthly and annual rainfall totals were calculated by summing daily precipitation values within their respective calendar periods. The resulting monthly dataset comprised 492 observations per state, while the annual dataset contained 41 observations per state.

Data-quality control involved examining temporal completeness, missing observations, duplicate dates, invalid precipitation values, and consistency between daily, monthly, and annual rainfall aggregations. The supplied datasets contained the expected number of daily, monthly, and annual records. Rainfall totals reconstructed from daily observations were compared with the corresponding monthly rainfall records to assess temporal aggregation consistency.

Annual maximum daily rainfall (AMAX-D) was defined as the highest daily precipitation value recorded during each calendar year. Annual maximum monthly rainfall (AMAX-M) was defined as the highest monthly accumulated rainfall within the same calendar year. These two extreme-rainfall indices were analyzed independently because they represent different precipitation accumulation periods and hydrometeorological characteristics.

The temporal aggregation and basic data-quality measures were computed as follows:

$$R_{m,\gamma} = \Sigma[d \in (m,y)]\ r_d \quad (1)$$

$$A_\gamma = \Sigma[d \in y]\ r_d = \Sigma[m = 1 \text{ to } 12]\ R_{m,\gamma} \quad (2)$$

$$M^d_\gamma = \max[d \in y](r_d) \quad (3)$$

$$M^m_\gamma = \max[m = 1,\ldots,12](R_{m,\gamma}) \quad (4)$$

$$M^m_\gamma = \max[m = 1,\ldots,12](R_{m,\gamma}) \quad (5)$$

where r_d is daily rainfall, $R_{m,\gamma}$ is monthly rainfall in month m of year y, A_γ is annual rainfall, M^d_γ and M^m_γ are annual maximum daily and monthly rainfall, n_γ is the number of observed days, and N_γ is the expected number of calendar days in year y.

Descriptive statistics were calculated using:

$$\bar{x} = (1/n)\ \Sigma_i\ x_i \quad (6)$$

$$s = \sqrt{[\Sigma_i(x_i - \bar{x})^2/(n-1)]} \quad (7)$$

$$CV\ (\%) = 100s/\bar{x} \quad (8)$$

$$g_1 = [n/((n-1)(n-2))]\ \Sigma_i[(x_i - \bar{x})/s]^3 \quad (9)$$

Table 1 presents the descriptive statistics of CHIRPS daily rainfall for Bayelsa, Rivers, and Delta States during 1983–2023. Each state contains 14,975 daily observations, corresponding to the expected number of calendar days over the 41-year study period. Bayelsa recorded the highest mean daily rainfall of 8.513 mm/day, followed by Rivers at 7.576 mm/day and Delta at 6.554 mm/day. The median daily rainfall values were consistently lower than their respective means, indicating positively skewed rainfall distributions.

Table 1. Descriptive statistics of CHIRPS daily rainfall across Bayelsa, Rivers, and Delta States, Niger Delta, Nigeria (1983–2023).

Parameter	Bayelsa	Rivers	Delta
Longitude (°E)	6.104	6.926	5.964
Latitude (°N)	4.763	4.857	5.711
Daily observations	14,975	14,975	14,975
Mean rainfall (mm/day)	8.513	7.576	6.554
Median rainfall (mm/day)	4.146	3.868	2.795
Standard deviation (mm/day)	11.409	10.086	9.053
Minimum rainfall (mm/day)	0.000	0.000	0.000
Maximum rainfall (mm/day)	125.367	126.731	93.724
Skewness	2.313	2.416	2.245
Coefficient of variation (%)	134.017	133.134	138.135

The daily standard deviations were 11.409 mm in Bayelsa, 10.086 mm in Rivers, and 9.053 mm in Delta, demonstrating considerable variability in daily precipitation. The highest observed daily rainfall occurred in Rivers (126.731 mm), followed by Bayelsa (125.367 mm) and Delta (93.724 mm).

All three states exhibited pronounced positive skewness, ranging from 2.245 in Delta to 2.416 in Rivers. This distributional asymmetry reflects the presence of relatively infrequent high-rainfall observations. The coefficients of variation exceeded 130% in all states, with Delta exhibiting the highest relative variability (138.135%), followed by Bayelsa (134.017%) and Rivers (133.134%). These findings demonstrate substantial differences in rainfall magnitude and variability across the three states. Although Bayelsa recorded the highest average daily rainfall, Rivers exhibited the highest observed daily extreme. This distinction emphasizes the importance of analyzing rainfall accumulation and extreme precipitation separately.

The observed positive skewness and high variability provide a basis for investigating upper-tail rainfall characteristics using extreme-value probability distributions, including Gumbel, Log-Pearson Type III, and Generalized Extreme Value models. Model suitability, however, requires independent assessment using goodness-of-fit statistics and uncertainty estimates.

2.2.2. Annual Rainfall Trend

Linear regression was employed to assess the magnitude and direction of temporal changes in annual rainfall across Bayelsa, Rivers, and Delta States during 1983–2023. The analysis was performed independently for each state using annual rainfall totals derived from CHIRPS daily precipitation data.

Ordinary least squares (OLS) regression was used to estimate the linear relationship between annual rainfall and time. The regression model was expressed as:

$$Y_t = mt + b + \varepsilon_t \quad (10)$$

where Y_t is annual rainfall (mm), t is the calendar year, m is the regression slope (mm/year), b is the intercept, ε_t and is the regression error.

2.3. The Bayesian Gumbel Inference

Bayesian inference provides a probabilistic framework for estimating the parameters of extreme-value distributions while explicitly accounting for parameter uncertainty. In this study, the Bayesian Gumbel framework was formulated for annual maximum daily

rainfall (AMAX-D) and annual maximum monthly rainfall (AMAX-M) in Bayelsa, Rivers, and Delta States during 1983–2023.

The Gumbel distribution is characterized by a location parameter, μ, and a strictly positive scale parameter, β. Separate models were specified for each state and rainfall accumulation period to account for differences in extreme-rainfall magnitude and variability.

2.3.1. Bayesian Model Specification

Let x = $(x_1, x_2, \ldots x_n)$ represent the annual rainfall maxima, where n = 41 for each state and accumulation period.

Bayesian inference follows the Bayes' theorem:

$$\boldsymbol{p(\theta \mid \mathbf{x}) \propto p(\mathbf{x} \mid \theta) p(\theta)} \quad (11)$$

where $\theta = (\mu, \beta)$ denotes the parameter vector , $p(\boldsymbol{\theta} \mid \mathbf{x})$ is the posterior distribution, $\mathrm{p}(\mathbf{x} \mid \boldsymbol{\theta})$ is the likelihood function, and $p(\boldsymbol{\theta})$ is the prior distribution.

Assuming independent annual maxima, the Gumbel likelihood function is:

$$\boldsymbol{L(\mu, \beta \mid \mathbf{x}) = \prod_{i=1}^{n} \frac{1}{\beta} exp[-z_i - exp(-z_i)]} \quad (12)$$

where the standardized variable is:

$$\boldsymbol{z_i = \frac{x_i - \mu}{\beta}, \qquad \beta > 0} \quad (13)$$

Weakly informative prior distributions are represented as:

$$\boldsymbol{\mu \sim \mathcal{N}(m_0, s_0^2)} \quad (14)$$

$$\boldsymbol{\beta \sim \mathbf{HalfNormal}(\sigma_\beta)} \quad (15)$$

Here, m_0 is the prior mean for the location parameter, S_0 is its prior standard deviation, and σ_β is the scale parameter of the half-normal prior.

The prior hyperparameters should be specified separately for daily and monthly rainfall maxima because their magnitudes differ substantially.

2.3.2. Posterior Sampling and Convergence Diagnostics

The proposed Bayesian estimation procedure uses four independent Markov chain Monte Carlo (MCMC) chains. Convergence and sampling efficiency are assessed using the rank-normalized potential scale reduction statistic, effective sample size (ESS), trace plots, and divergent-transition diagnostics where applicable.

The conventional potential scale reduction statistic is expressed as:

$$\boldsymbol{\widehat{R} = \sqrt{\frac{\widehat{V}}{W}}} \quad (16)$$

where $\boldsymbol{W}$ represents the within-chain variance and $\boldsymbol{\widehat{V}}$ is the estimated marginal posterior variance. Equation (16) represents the conventional variance-based statistic. Rank-normalized and folded versions provide more robust convergence diagnostics.

The effective sample size is approximated by:

$$\boldsymbol{ESS \approx \frac{MN}{1 + 2\sum_{k=1}^{\infty} \widehat{\rho}_k}}. \quad (17)$$

where $\boldsymbol{M}$ is the number of MCMC chains, $\boldsymbol{N}$ is the number of retained draws per chain, and $\boldsymbol{\widehat{\rho}_k}$ is the estimated lag-k autocorrelation.

Values of rank-normalized $\widehat{\boldsymbol{R}}$ close to 1.00, particularly below 1.01, together with sufficiently large bulk and tail ESS, provide evidence of satisfactory sampling behaviour. These criteria should be assessed alongside trace plots and other sampler diagnostics.

2.3.3. Posterior Predictive Assessment

Posterior predictive checks evaluate the extent to which the fitted Bayesian Gumbel model reproduces the statistical characteristics of observed annual rainfall maxima.

For posterior draw **s**, a replicated observation is generated as:

$$\tilde{\boldsymbol{x}}_{\boldsymbol{i}}^{(\boldsymbol{s})} \sim \mathbf{Gumbel}\left(\boldsymbol{\mu}^{(\boldsymbol{s})}, \boldsymbol{\beta}^{(\boldsymbol{s})}\right) \quad (18)$$

where $\tilde{\boldsymbol{x}}_{\boldsymbol{i}}^{(\boldsymbol{s})}$ is a simulated annual rainfall maximum, while $\boldsymbol{\mu}^{(\boldsymbol{s})}$ and $\boldsymbol{\beta}^{(\boldsymbol{s})}$ are the location and scale parameters obtained from posterior draw **s**.

Model adequacy is evaluated by comparing the observed and replicated rainfall distributions, including their means, dispersion, upper-tail behaviour, and extreme quantiles.

2.3.4. Bayesian Rainfall Return-Level Estimation

Bayesian rainfall return levels are calculated using the posterior distributions of the Gumbel location and scale parameters.

For return period **T > 1**, the return level corresponding to posterior draw s is:

$$\boldsymbol{x}_{\boldsymbol{T}}^{(\boldsymbol{s})} = \boldsymbol{\mu}^{(\boldsymbol{s})} - \boldsymbol{\beta}^{(\boldsymbol{s})} \ln\left[-\ln\left(1 - \frac{1}{T}\right)\right] \quad (19)$$

where $x_T^{(s)}$ represents the estimated rainfall return level for return period T, $\mu^{(s)}$ is the posterior location parameter, and $\beta^{(s)}$ is the posterior scale parameter.

The posterior distribution of the return level is obtained by applying Equation (19) to all retained posterior draws. Posterior means and medians summarize the central estimates, while the 2.5th and 97.5th percentiles define the equal-tailed 95% Bayesian credible interval. We evaluate return levels for recurrence intervals of 2, 5, 10, 20, 50, and 100 years. Because the observational record contains 41 annual maxima per state, the 50-year and 100-year return levels involve extrapolation beyond the available observation period.

Uncertainty generally increases for longer return periods because estimates become increasingly sensitive to the fitted distribution's upper-tail behaviour and parameter uncertainty. The resulting Bayesian credible intervals describe uncertainty in the estimated return levels conditional on the assumed model and priors. They differ conceptually from frequentist confidence intervals and do not automatically account for uncertainty from alternative probability distributions or non-stationary.

2.4. Peaks-Over-Threshold (POT) and Generalized Pareto Distribution (GPD) Analysis

The Peaks-Over-Threshold (POT) approach was employed to characterize extreme daily rainfall events in Bayelsa, Rivers, and Delta States during the 1983–2023 study period. The method identifies rainfall observations exceeding a specified high threshold and models the corresponding exceedance magnitudes using the Generalized Pareto Distribution (GPD). Unlike the block-maxima approach, which retains one maximum observation per year, the POT method incorporates multiple extreme-rainfall events within individual years, thereby providing additional information on the magnitude and frequency of rainfall extremes. Daily rainfall observations were obtained from the Climate Hazards Group InfraRed Precipitation with Station Data (CHIRPS) dataset. The analysis

was conducted separately for each state to account for differences in rainfall characteristics and extreme-event occurrence.

Empirical rainfall thresholds corresponding to the 90th, 92.5th, 95th, 97.5th, and 99th percentiles were evaluated to investigate the sensitivity of fitted GPD parameters to threshold selection. The 95th percentile was adopted as the principal threshold for the final POT analysis. The corresponding state-specific thresholds were 31.65 mm day^{-1} for Bayelsa, 27.43 mm day^{-1} for Rivers, and 25.17 mm day^{-1} for Delta. The threshold-sensitivity analysis was initially performed using raw rainfall exceedances before declustering. The fitted GPD shape and scale parameters were examined across candidate thresholds to assess their stability and identify potential sensitivity associated with increasing threshold magnitudes and decreasing sample sizes.

Because consecutive rainfall exceedances often occur within the same meteorological event, temporal dependence was addressed using a three-day run-length declustering procedure. Exceedances separated by fewer than three consecutive non-exceedance days were assigned to the same cluster, and the maximum rainfall exceedance within each cluster was retained as the representative event magnitude. At the selected 95th-percentile thresholds, each state recorded 749 raw exceedances. Following declustering, 470 approximately independent rainfall events were retained for Bayelsa, 515 for Rivers, and 494 for Delta. These correspond to reductions of approximately 37.2%, 31.2%, and 34.0%, respectively.

The GPD was fitted to the excess rainfall magnitudes obtained from the declustered event maxima, with the location parameter fixed at zero. The fitted distribution was characterized by its shape and scale parameters. The shape parameter describes the behaviour of the upper tail, while the scale parameter represents the dispersion of exceedance magnitudes. The final fitted GPD shape parameters were 0.0182 for Bayelsa, 0.0232 for Rivers, and −0.0194 for Delta. The corresponding scale parameters were 13.71 mm, 12.47 mm, and 10.84 mm, respectively. These estimates were used for state-specific extreme-rainfall return-level calculations.

Model adequacy was assessed graphically using quantile–quantile (Q-Q) and probability–probability (P-P) diagnostics. The Q-Q plots compared observed declustered excess quantiles with theoretical GPD quantiles, while the P-P plots compared empirical cumulative probabilities with fitted cumulative probabilities. Departures from the diagonal reference lines were examined to identify potential discrepancies between the empirical and theoretical distributions, particularly in the upper tails. The annual occurrence rate of declustered extreme-rainfall events was calculated by dividing the number of retained events by the 41-year study duration. The resulting event rates were approximately 11.46, 12.56, and 12.05 events per year for Bayelsa, Rivers, and Delta, respectively.

Rainfall return levels were estimated for recurrence intervals of 2, 5, 10, 25, 50, and 100 years using the selected thresholds, fitted GPD parameters, and declustered event-occurrence rates. The return levels represent rainfall magnitudes associated with specified average exceedance frequencies under the assumed stationary POT-GPD framework. The estimated return levels describe extreme precipitation hazards rather than direct predictions of floodwater levels, inundation extent, or economic losses. Their interpretation therefore requires consideration of hydrological conditions, drainage characteristics, catchment response, and uncertainty associated with statistical extrapolation.

Threshold exceedance is given as:

$$Y = X - u, \qquad X > u \tag{20}$$

The Generalized Pareto cumulative distribution function is

$$H(y) = 1 - \left(1 + \frac{\xi y}{\beta}\right)^{-1/\xi} \quad (21)$$

where $\xi \neq 0, \beta > 0, 1 + \frac{\xi y}{\beta} > 0$

The Annual exceedance-event rate is given as

$$\lambda = \frac{N_u}{N_{\text{years}}} \quad (22)$$

Here, N_u represents the number of declustered exceedance events.

The POT-GPD return level for nonzero shape parameter is:

$$x_T = u + \frac{\beta}{\xi}\left[(\lambda T)^{\xi} - 1\right] \quad (23)$$

POT-GPD return level for zero shape parameter becomes:

$$x_T = u + \beta \ln(\lambda T) \quad (24)$$

Similarly, the Mean residual life

$$e(u) = E[X - u \mid X > u] \approx \frac{1}{N_u}\sum_{i:X_i>u}(X_i - u) \quad (25)$$

2.5. Non-Stationary Generalized Extreme Value Sensitivity Analysis

Stationary and time-varying GEV specifications are described as candidate sensitivity analyses. A claim of improved non-stationary performance requires CHIRPS-specific maximum-likelihood fits, parameter uncertainty, AIC/BIC and likelihood-ratio results. An annual-total trend alone does not establish a significant trend in annual maxima.

The Stationary GEV cumulative distribution function is given as**:**

$$\boldsymbol{G(x) = \exp\left\{-\left[1 + \xi\left(\frac{x-\mu}{\sigma}\right)\right]^{-1/\xi}\right\}} \quad (26)$$

where $\boldsymbol{\sigma > 0, \xi \neq 0}$**, and** $\boldsymbol{1 + \xi(x - \mu)/\sigma > 0}$

Time-varying GEV location parameter:

$$\boldsymbol{\mu}(t) = \mu_0 + \mu_1\left(t - \bar{t}\right) \quad (27)$$

The likelihood-ratio statistic is given as:

$$LR = 2\left[\ln\left(\hat{L}_{NS}\right) - \ln\left(\hat{L}_S\right)\right] \quad (28)$$

2.6. Classical Gumbel and Log-Pearson Type III Frequency Analysis

The Gumbel distribution is used to model extreme values, such as the highest rainfall levels or flood peaks. Additionally, the Gumbel distribution is applied to evaluate monthly and annual maximums of 24 h rainfall and basin water yield. Known as the type I extreme-value distribution, the Gumbel distribution was introduced by Gumbel [42] and is a valuable tool in extreme-value analysis, especially in hydrology, for assessing rainfall frequency, intensity, and return periods.

Similarly, the Log-Pearson Type III distribution is commonly used in hydrology for flood frequency analysis and is based on the Pearson Type III distribution applied to the logarithms of the data. It is particularly valuable for estimating flood frequency and understanding extreme events in water resources management, making it essential for predicting the behaviour of hydrological processes over time.

The classical analysis fits the two-parameter Gumbel distribution and LP3 distribution separately to annual maximum daily and annual maximum monthly rainfall. Gumbel parameters were estimated by maximum likelihood. LP3 was fitted to log10-transformed annual maxima using the Pearson Type III distribution. Return levels were estimated for 2, 5, 10, 25, 50 and 100 years. Model adequacy was evaluated with Q-Q based RMSE, MAE, Nash–Sutcliffe efficiency (NSE) and correlation, together with parametric-bootstrap Kolmogorov–Smirnov and Anderson–Darling tests that refit parameters in each bootstrap replicate. Classical sampling uncertainty should be quantified by parametric bootstrap confidence intervals with parameter refitting, consistent with the bootstrap procedure used for the K-S and A-D goodness-of-fit tests.

Gumbel cumulative distribution function becomes:

$$F(x) = \exp\left\{-\exp\left[-\frac{x-\mu}{\beta}\right]\right\} \tag{29}$$

where $\beta > 0$.

The LP3 return quantile on the logarithmic scale is

$$y_T = F_{\mathrm{PIII}}^{-1}\left(1-\frac{1}{T};\gamma,\mu_Y,\sigma_Y\right) \tag{30}$$

This follows:

$$x_T = 10^{y_T} \tag{31}$$

Model-selection and predictive-fit statistics were calculated using:

Akaike Information Criterion

$$AIC = 2k - 2\ln\left(\hat{L}\right) \tag{32}$$

Bayesian Information Criterion

$$BIC = k\ln(n) - 2\ln\left(\hat{L}\right) \tag{33}$$

2.7. Model Performance Evaluation

To evaluate the performance of the hydrological models used in the study, three commonly employed evaluation constraints, namely the Nash–Sutcliffe Efficiency (NSE), the Root Mean Squared Error (RMSE), and Mean Absolute Error (MAE), were adopted to assess the goodness of fit between the simulated and the observed values. The three model evaluation metrics are discussed as follows

Quantile–Quantile Root Mean Square Error

$$RMSE = \sqrt{\frac{1}{n}\sum_{i=1}^{n}(x_i - q_i)^2} \tag{34}$$

Quantile–Quantile Mean Absolute Error

$$MAE = \frac{1}{n}\sum_{i=1}^{n}|x_i - q_i| \tag{35}$$

The Nash–Sutcliffe Efficiency

$$NSE = 1 - \frac{\sum_{i=1}^{n}(x_i - q_i)^2}{\sum_{i=1}^{n}(x_i - \overline{x})^2} \tag{36}$$

The Kolmogorov–Smirnov and Anderson–Darling statistics were:

$$D = \sup_x |F_n(x) - F(x)| \tag{37}$$

Anderson–Darling test statistic is given as:

$$A^2 = -n - \frac{1}{n}\sum_{i=1}^{n}(2i-1)\left[\ln F\left(x_{(i)}\right) + \ln\left(1 - F\left(x_{(n+1-i)}\right)\right)\right] \quad (38)$$

2.8. Homogeneity Test

To improve data reliability, we analyzed the annual and monthly rainfall data using two tests: Pettitt's test and the Standardized Normal Homogeneity Test (SNHT). These tests check for shifts in the data. Pettitt's test identifies abrupt changes by computing the highest rank-based U statistic over the series, whereas the SNHT assesses changes by comparing average deviations before and after specific points. These tests are important because they help account for factors that might affect the dataset, such as relocating observation stations, urban growth, population increases, and natural events. Conducting these homogeneity tests strengthens the credibility of our climate and hydrology models

2.8.1. Standard Normal Homogeneity Test

The SNHT is a common method in climate research, developed by Alexandersson. It effectively identifies time-series change points, particularly those attributable to instrument changes or site relocations. Alexandersson [43] identifies a reference point in the series at a breakpoint and calculates the statistic accordingly, as expressed below:

SNHT statistic for a candidate breakpoint

$$T(\boldsymbol{t}) = t\overline{Z}_1^{\,2} + (n-t)\overline{Z}_2^{\,2} \quad (39)$$

Standardized rainfall observations:

$$Z_i = \frac{X_i - \overline{X}}{s} \quad (40)$$

Maximum SNHT statistic

$$T_{\max} = \max_{1 \le t < n} T(t) \quad (41)$$

2.8.2. Pettitt Test (Change-Point Detection Test)

This is a nonparametric test, developed by [44], to identify changes in the breakpoint in rainfall data and to determine whether they occur on a monthly or annual timescale. The test does not require any assumption of normality. The statistics are given as follows:

The Pettitt rank-based statistic is given as:

$$U_t = \sum_{i=1}^{t}\sum_{j=t+1}^{n} \operatorname{sgn}\left(X_i - X_j\right) \quad (42)$$

Pettitt maximum test statistic:

$$K = \max_{1 \le t < n} |U_t| \quad (43)$$

Approximate Pettitt *p*-value:

$$p \approx 2\exp\left(-\frac{6K^2}{n^3 + n^2}\right) \quad (44)$$

3. Results

This section presents the results of the extreme-rainfall analysis conducted for Bayelsa, Rivers, and Delta States in the Niger Delta, Nigeria, using Climate Hazards Group InfraRed Precipitation with Station Data (CHIRPS) observations covering 1983–2023.

The analysis of CHIRPS-derived annual rainfall totals from 1983 to 2023 as shown in Figure 3 reveals substantial interannual variability across Bayelsa, Rivers, and Delta States in the Niger Delta region of Nigeria. Rainfall totals fluctuate considerably throughout the 41-year study period, reflecting variations in annual precipitation across the three states. Bayelsa generally records the highest annual rainfall totals, ranging from approximately 2200 to 3800 mm, followed by Rivers, with totals between 2100 and 3350 mm, and Delta, with totals ranging from 1900 to 2980 mm. Pronounced rainfall maxima occurred in 1995, 1999, and 2009, particularly in Bayelsa, while relatively low rainfall totals were recorded in 2001 and 2015 across the three states. These fluctuations indicate considerable interannual rainfall variability, with alternating wetter and drier years rather than a consistent increase or decrease in annual precipitation.

Ordinary least squares linear regression indicates weak negative rainfall trends across all three states. Bayelsa exhibits the largest estimated decline of −3.69 mm/year (p = 0.469, R^2 = 0.014), followed by Delta at −1.73 mm/year (p = 0.625, R^2 = 0.006) and Rivers at −0.95 mm/year (p = 0.806, R^2 = 0.002) as shown in Table 2. These trends correspond to estimated decreases of 36.9 mm, 17.3 mm, and 9.5 mm per decade, respectively. However, none of the estimated linear trends is statistically significant at the 5% significance level (p > 0.05). The low coefficients of determination indicate that linear time trends explain only approximately 0.2–1.4% of the observed annual rainfall variability. This suggests that year-to-year fluctuations dominate the rainfall records, while the estimated long-term linear changes remain small relative to interannual variability.

Table 2. Comparison of annual rainfall trends derived from ordinary least squares regression, the Mann–Kendall test, and Sen's slope estimation, including 95% confidence intervals, for Bayelsa, Rivers, and Delta States (1983–2023).

State	OLS Slope (mm/y)	OLS p	Sen Slope (mm/y)	Sen 95% CI	MK Z	MK p
Bayelsa	−3.69	0.469	−3.04	−13.56 to 6.96	−0.573	0.567
Rivers	−0.95	0.806	0.59	−8.14 to 7.77	0.056	0.955
Delta	−1.73	0.625	−1.76	−9.41 to 6.53	−0.393	0.694

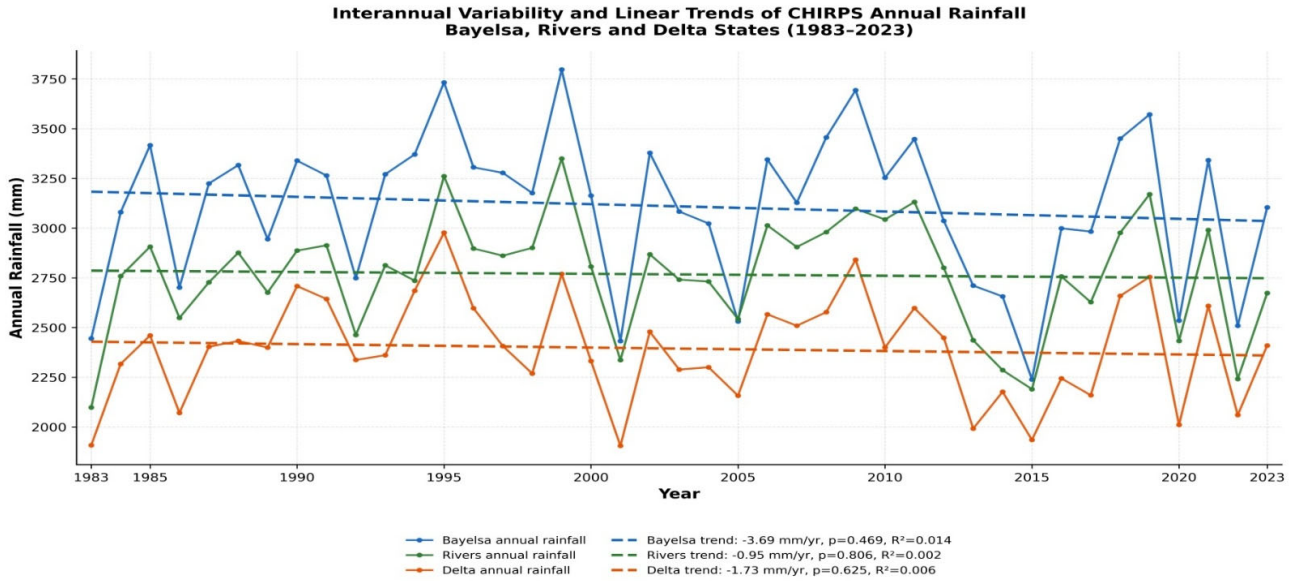


Figure 3. Interannual variability and linear trends of annual rainfall in Bayelsa, Rivers, and Delta States, Nigeria (1983–2023).

The interannual rainfall variability analysis provides insufficient statistical evidence of a systematic linear increase or decrease in annual rainfall totals across the three states during 1983–2023. Nevertheless, statistically non-significant trends do not establish rainfall stationary or exclude changes in seasonal rainfall distribution, extreme precipitation intensity, or rainfall-event frequency. Furthermore, the reported *p*-values rely on the assumption of independent regression errors, which requires verification through residual autocorrelation analysis.

The substantial interannual rainfall variability highlights the importance of examining rainfall extremes independently of annual precipitation totals. Years with relatively moderate annual rainfall might still experience intense short-duration rainfall events capable of contributing to flooding, drainage-system overload, and coastal inundation. Therefore, the annual rainfall analysis provides a climatic baseline for the subsequent examination of annual maximum daily and monthly rainfall, probability distribution models, and extreme-rainfall return levels. These additional analyses are necessary to characterize extreme precipitation hazards and assess their implications for flood risk and coastal vulnerability in Bayelsa, Rivers, and Delta States.

The monthly rainfall climatology is shown in Figure 4 which illustrates the long-term mean monthly rainfall distribution across Bayelsa, Delta, and Rivers States, derived from CHIRPS precipitation data for 1983–2023. The three states exhibit a pronounced seasonal rainfall cycle, characterized by relatively low rainfall totals during January and February, followed by a progressive increase toward the primary rainfall maximum in June–July. Rainfall decreases in August before increasing again in September, producing a bimodal seasonal pattern. Monthly rainfall subsequently declines toward December. Bayelsa generally records the highest monthly rainfall totals, followed by Rivers and Delta. This spatial variation reflects differences in rainfall distribution across the three coastal states, although the figure alone does not establish the physical causes of these differences.

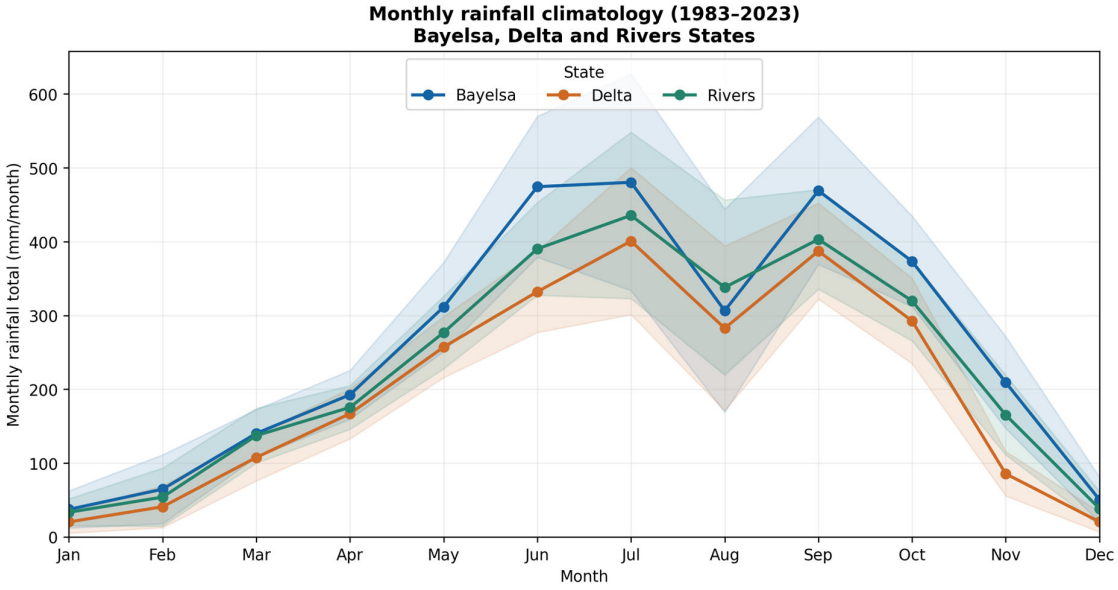


Figure 4. Monthly rainfall climatology for Bayelsa, Delta, and Rivers States (1983–2023).

The shaded bands represent the climatological monthly mean ± 1 interannual standard deviation, calculated from the 41 monthly totals for each calendar month. These bands quantify year-to-year rainfall variability rather than uncertainty in the estimated climatological mean. Overlapping standard-deviation bands do not demonstrate statistical equivalence among states. The relative August rainfall minimum is consistent

with the seasonal rainfall reduction commonly observed in parts of southern Nigeria. However, Figure 4 provides descriptive evidence of this pattern rather than a formal statistical test of its significance.

Table 3 shows that the three state-level series contain 14,975 valid daily observations, with no missing dates, duplicates, or negative precipitation values. The 100% temporal completeness allowed all 41 calendar years to be retained without applying an incomplete-year exclusion threshold. These findings establish a consistent temporal basis for the trend and extreme-value analyses.

Table 3. Completeness and quality-control assessment of state-level CHIRPS daily rainfall series for Bayelsa, Rivers, and Delta States, Niger Delta, Nigeria (1983–2023). Counts describe the aggregated state-level time series rather than individual CHIRPS grid-cell observations.

State	Expected Days	Valid Days	Missing	Duplicates	Negative	Completeness
Bayelsa	14,975	14,975	0	0	0	100.0%
Rivers	14,975	14,975	0	0	0	100.0%
Delta	14,975	14,975	0	0	0	100.0%

3.1. Spatial Analysis of Precipitation Variability

Spatial precipitation variability is examined using four complementary gridded CHIRPS maps. Mean annual rainfall describes the long-term spatial distribution of accumulated precipitation over four decades (1983–1993, 1993–2003, 2003–2013 and 2013–2023). The annual rainfall trend map represents the fitted slope in mm/year at each mapped cell. The interannual standard-deviation map measures absolute year-to-year variation in annual totals, while the coefficient-of-variation map expresses the standard deviation as a percentage of the local annual mean. These metrics correspond to different aspect of the spatial analysis and should not be treated as interchangeable. The four indicators provide complementary information on the magnitude, direction of change, and temporal variability of rainfall across the study area.

The mean annual rainfall map (Figure 5a) reveals a pronounced spatial gradient, with higher precipitation totals concentrated predominantly in the southern coastal and southwestern portions of the study area. Rainfall generally decreases toward the northern and inland regions. This distribution is consistent with the influence of maritime moisture and seasonal monsoon circulation over southern Nigeria. However, attributing these spatial differences to specific atmospheric mechanisms requires additional meteorological analysis.

The annual rainfall trend map (Figure 5b) demonstrates spatially heterogeneous changes during the study period. Negative rainfall trends dominate several coastal and southwestern locations, particularly within parts of Bayelsa and southern Delta, while localized positive trends appear in some northern and inland areas. These contrasting patterns indicate that rainfall changes are not spatially uniform across the three states. Nevertheless, the mapped slopes represent estimated changes in annual rainfall rather than statistically confirmed trends, since pixel-level significance testing was not performed.

The interannual standard-deviation map (Figure 5c) indicates considerable geographical variation in the absolute variability of annual rainfall totals. Higher standard deviations occur mainly across southern and southwestern coastal areas, while comparatively lower values characterize several northern and inland locations. This pattern suggests that locations receiving greater annual rainfall also tend to exhibit larger absolute year-to-year fluctuations. However, standard deviation alone does not establish changes in extreme-rainfall frequency or intensity.

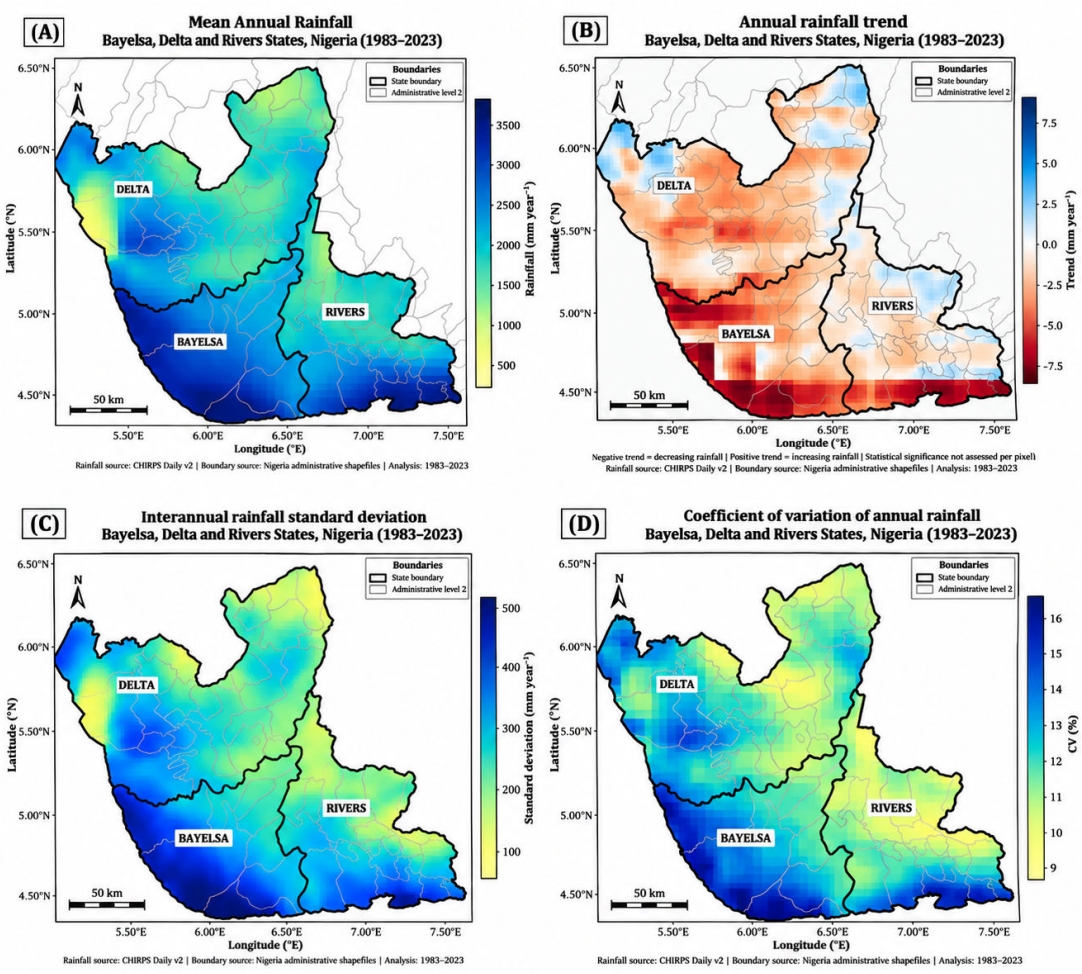


Figure 5. Spatial rainfall characteristics for Bayelsa, Delta and Rivers States, 1983–2023 using CHIRPS data: (**A**) mean annual rainfall (mm/year), (**B**) linear annual rainfall trend (mm/year per year), (**C**) interannual standard deviation of annual totals (mm/year), and (**D**) coefficient of variation (%).

The coefficient of variation map (Figure 5d) provides a normalized measure of interannual rainfall variability relative to the local mean. Values range approximately from 9% to 17%, with relatively elevated coefficients in parts of the southwestern and coastal areas and lower values across portions of the northern interior. Unlike standard deviation, the coefficient of variation permits comparison of relative rainfall variability among locations with different mean rainfall totals. The spatial differences therefore indicate varying degrees of interannual rainfall consistency across the study domain.

Taken together, the four maps demonstrate substantial spatial heterogeneity in rainfall magnitude and variability across Bayelsa, Delta, and Rivers States. The coastal and southwestern areas generally experience higher annual precipitation and greater absolute variability, while estimated rainfall trends vary geographically. Importantly, the pixel-level patterns differ in spatial support from the state-aggregated annual rainfall trends discussed previously. Therefore, localized positive or negative slopes should not be interpreted as contradicting the statistically nonsignificant state-level trends.

These analyses provide a spatial context for understanding precipitation variability in the Niger Delta region. However, the analysis does not establish statistically significant pixel-level trends or changes in extreme-rainfall return levels.

3.2. Bayesian Gumbel Inference

Bayesian Gumbel inference was applied to characterize uncertainty in the location (μ) and scale (β) parameters of annual maximum daily and monthly rainfall distributions. The approach combines the Gumbel likelihood with specified prior distributions to estimate posterior parameter uncertainty and assess extreme-rainfall characteristics. The reported posterior summaries include parameter means, standard deviations, 95% highest-density intervals (HDIs), and Markov Chain Monte Carlo (MCMC) convergence diagnostics, including R-hat, effective sample sizes, and divergent transitions.

Table 4 presents the Bayesian Gumbel posterior estimates of location (μ) and scale (β) parameters for annual maximum daily and monthly rainfall across Bayelsa, Rivers, and Delta States during 1983–2023. The results reveal consistent spatial differences in the fitted extreme-rainfall distributions.

Table 4. Bayesian Gumbel parameter estimates for annual maximum daily and monthly rainfall (1983–2023).

State	Series	Parameter	Mean ± SD (mm)	95% HDI (mm)	Bulk ESS	R-Hat
Bayelsa	Daily	μ	65.324 ± 2.687	60.017–70.544	4065	1.00
Bayelsa	Daily	β	16.299 ± 2.115	12.418–20.412	3833	1.00
Bayelsa	Monthly	μ	522.238 ± 14.464	492.458–549.638	4087	1.00
Bayelsa	Monthly	β	88.270 ± 10.895	68.605–110.450	4384	1.00
Rivers	Daily	μ	61.631 ± 2.286	57.099–66.167	4124	1.00
Rivers	Daily	β	13.694 ± 1.805	10.448–17.306	3409	1.00
Rivers	Monthly	μ	455.548 ± 11.434	432.468–477.043	3966	1.00
Rivers	Monthly	β	69.367 ± 8.499	53.800–86.255	4175	1.00
Delta	Daily	μ	50.896 ± 2.000	46.926–54.701	4045	1.00
Delta	Daily	β	12.018 ± 1.601	9.006–15.085	4210	1.00
Delta	Monthly	μ	420.447 ± 9.983	400.727–440.263	3662	1.00
Delta	Monthly	β	60.095 ± 7.430	45.912–74.494	3706	1.00

For annual maximum daily rainfall, Bayelsa recorded the highest posterior mean location parameter (65.324 ± 2.687 mm), followed by Rivers (61.631 ± 2.286 mm) and Delta (50.896 ± 2.000 mm). Similarly, the scale parameter was highest in Bayelsa (16.299 ± 2.115 mm), compared with Rivers (13.694 ± 1.805 mm) and Delta (12.018 ± 1.601 mm). These estimates indicate higher fitted daily rainfall extremes and greater dispersion in Bayelsa, while Delta exhibited the lowest parameter estimates.

For annual maximum monthly rainfall, Bayelsa also recorded the highest posterior mean location parameter (522.238 ± 14.464 mm), followed by Rivers (455.548 ± 11.434 mm) and Delta (420.447 ± 9.983 mm). The corresponding scale parameters were 88.270 ± 10.895 mm, 69.367 ± 8.499 mm, and 60.095 ± 7.430 mm, respectively. This consistent ordering suggests greater fitted monthly extreme-rainfall magnitudes and variability in Bayelsa relative to Rivers and Delta.

The 95% highest-density intervals quantify uncertainty in the estimated parameters. Although the posterior means differ among states, overlapping intervals for some parameters indicate that the magnitude and credibility of pairwise differences require formal posterior comparison.

The MCMC convergence diagnostics indicate satisfactory sampling performance across all six models. R-hat values were reported as 1.00, while bulk effective sample sizes ranged from 3409 to 4384. Furthermore, all models recorded zero divergent transitions, supporting stable posterior sampling.

The result demonstrates a consistent spatial ordering of fitted extreme-rainfall characteristics, with Bayelsa exhibiting the highest posterior mean location and scale parameters, followed by Rivers and Delta. These results support state-specific extreme-rainfall assessment and provide a statistical basis for subsequent return-level estimation. Nevertheless, the parameter estimates alone do not establish temporal trends, causal mechanisms, or differences in flood risk across the study area. The posterior predictive checks for annual maximum daily rainfall in Bayelsa, Rivers, and Delta States for the study period 1983–2023 are shown in Figure 6 where observed distributions are compared with posterior predictive simulations from state-specific Bayesian Gumbel models.

Figure 6 presents posterior predictive checks for annual maximum daily rainfall in Bayelsa, Rivers, and Delta States during 1983–2023. The black curves represent the observed rainfall distributions, the orange dashed curves indicate the mean posterior predictive distributions, and the light-blue curves represent individual posterior predictive simulations. The results demonstrate generally satisfactory agreement between the observed and simulated distributions across the three states, indicating that the Bayesian Gumbel models reproduce the principal characteristics of annual maximum daily rainfall.

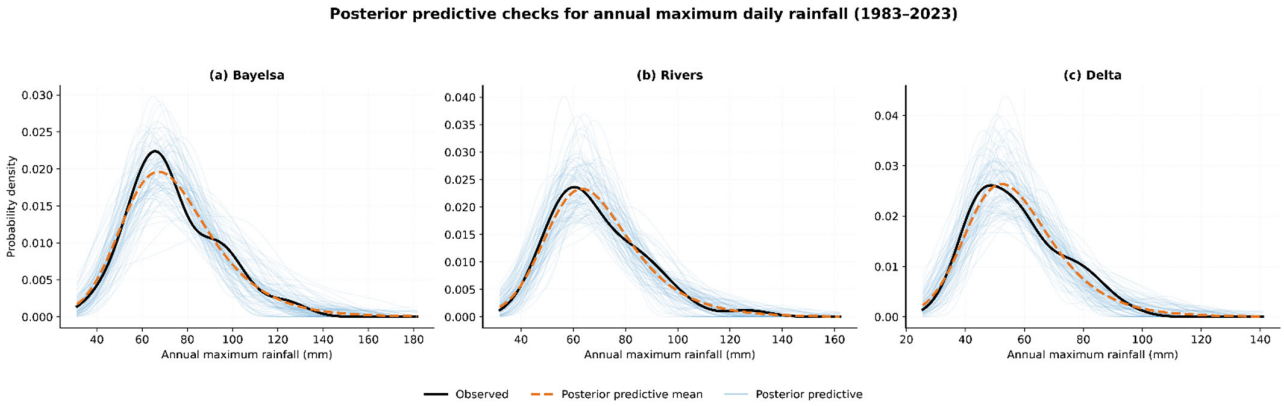


Figure 6. Posterior predictive check for annual maximum daily rainfall.

In Bayelsa State, the observed rainfall distribution exhibits a pronounced peak around 65–70 mm, followed by a progressively declining upper tail. The posterior predictive mean closely follows the observed distribution, although it produces a slightly lower and broader central peak. This suggests that the model adequately represents the central tendency and general variability of daily rainfall extremes, while smoothing some features of the empirical distribution.

In Rivers State, the observed and posterior predictive distributions show particularly close agreement around the dominant rainfall range of approximately 55–80 mm. The model reproduces the right-skewed structure of the observed annual maxima, although minor differences occur around the upper shoulder of the distribution. These differences suggest limited discrepancies in the representation of rainfall variability at higher intensities. Delta State also exhibits substantial agreement between the observed and simulated distributions. The observed distribution peaks near 50 mm, with a secondary shoulder toward higher rainfall intensities. The posterior predictive mean captures the dominant peak and overall right-skewed structure but smooths the secondary feature.

Across the three states, the overlapping posterior predictive curves indicate uncertainty in the estimated rainfall distributions. The visual agreement supports the use of state-specific Bayesian Gumbel models for describing annual maximum daily rainfall. However, these density-based checks primarily assess the overall distribution.

Figure 7 evaluates the posterior predictive performance of the Bayesian Gumbel models fitted to annual maximum monthly rainfall for the three states of Bayelsa, Delta and Rivers covering 1983–2023. The posterior predictive distributions generally reproduce the right-skewed characteristics of the observed monthly rainfall maxima. Nevertheless, differences between the observed and simulated density peaks indicate some limitations in representing the detailed shapes of the empirical distributions.

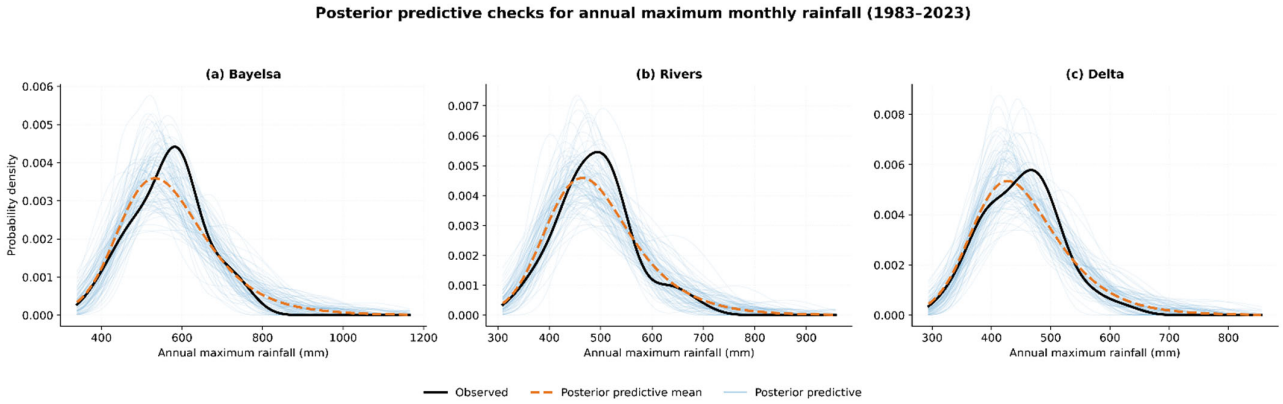


Figure 7. Posterior predictive check for annual maximum monthly rainfall.

For Bayelsa State, the observed distribution peaks around 570–590 mm, whereas the posterior predictive mean has a broader peak near 530–550 mm. The predictive distribution therefore assigns relatively greater density to lower monthly maxima than the observed density peak suggests. Despite this difference, the simulated curves encompass much of the observed distribution, including its declining upper tail. In Rivers State, the observed monthly rainfall distribution peaks around 490–510 mm, while the posterior predictive mean is centred slightly lower. The model captures the broad distributional structure and declining upper tail, although the observed curve displays a sharper central peak and local variations that are less pronounced in the simulated distribution. Delta State shows a similar pattern. The observed distribution has a pronounced peak near 460–480 mm, whereas the posterior predictive mean is broader and peaks at a somewhat lower rainfall amount. The simulated distributions reproduce the general asymmetry and upper-tail behaviour, but the differences in peak location and concentration indicate imperfect reproduction of the observed distribution. The three panels suggest that the Bayesian Gumbel models provide reasonable approximations to annual maximum monthly rainfall. However, the systematic differences between observed and predicted central peaks warrant further examination. These differences are particularly relevant because monthly rainfall extremes represent accumulated precipitation over longer periods and reflect the combined effects of rainfall frequency, persistence, and intensity.

Figure 8 illustrates the MCMC sampling trajectories for the Gumbel location (μ) and scale (β) parameters estimated from annual maximum daily rainfall in Bayelsa, Rivers, and Delta States with each panel displaying three independently sampled chains over 2000 retained posterior iterations. The trace plots exhibit substantial overlap among the four chains, with fluctuations around relatively stable central values throughout the sampling period. No sustained upward or downward drift is visually apparent. For Bayelsa State, the location parameter fluctuates predominantly around 65 mm, while the scale parameter remains centred near 16 mm. The four chains overlap throughout the sampling period, indicating consistent exploration of similar posterior regions.

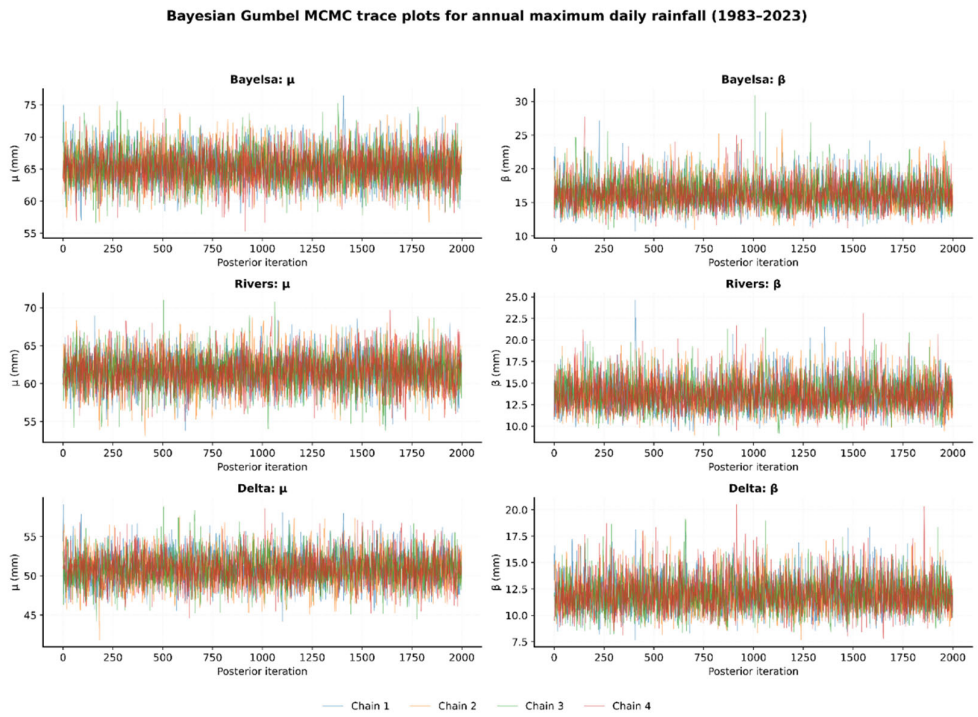


Figure 8. Bayesian Gumbel trace plots for annual maximum daily rainfall.

For Rivers State, the location parameter fluctuates around 62 mm, and the scale parameter around 14 mm. The chains display stable variability without persistent separation or obvious systematic trends. Delta State exhibits a location parameter centred near 51 mm and a scale parameter near 12 mm. The trace plots similarly show substantial overlap among chains and no clear evidence of prolonged sampling instability.

The relative positions of the sampled parameters indicate that Bayelsa has the highest estimated location and scale parameters, followed by Rivers and Delta. The location parameter reflects the position of the fitted Gumbel distribution, while the scale parameter describes its dispersion. Consequently, the higher Bayelsa parameter estimates suggest a fitted distribution shifted toward greater daily rainfall maxima and exhibiting greater dispersion.

The trace plots provide visual evidence of satisfactory chain mixing and approximate stationarity. Nevertheless, formal convergence assessment requires examination of rank-normalized R-hat statistics, effective sample sizes, and divergent transitions. Visual overlap alone is insufficient to confirm convergence.

Similarly, Figure 9 presents MCMC trace plots for the Gumbel location and scale parameters estimated from annual maximum monthly rainfall in Bayelsa, Rivers, and Delta States. The three chains for each parameter display substantial overlap and fluctuate around stable central values, with no obvious long-term trends or persistent separation. For Bayelsa State, the location parameter is centred near 522 mm, while the scale parameter fluctuates around 88 mm. The relatively broad variation in the scale parameter reflects uncertainty in the dispersion of monthly rainfall extremes**.**

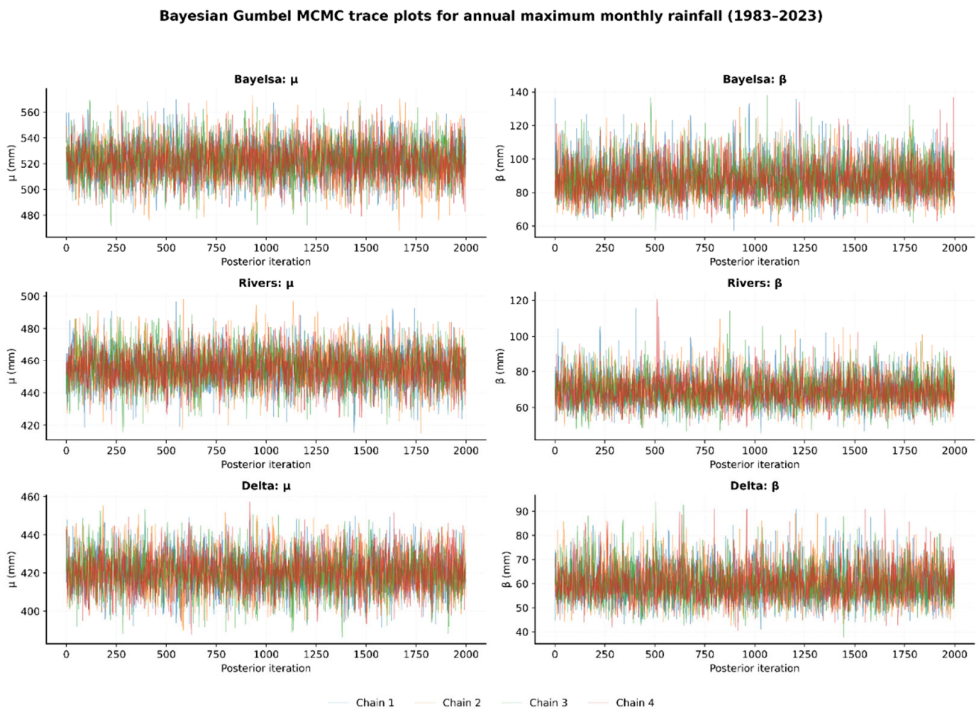


Figure 9. Bayesian Gumbel trace plots for annual maximum monthly rainfall.

Rivers State exhibits a location parameter centred near 456 mm and a scale parameter near 69 mm. The three chains overlap consistently, indicating visually stable posterior sampling behaviour. For Delta State, the location parameter fluctuates around 420 mm, while the scale parameter remains centred near 60 mm. The trace plots show comparable mixing behaviour across the chains.

The monthly results preserve the ordering observed for daily rainfall extremes, with Bayelsa displaying the highest fitted location and scale parameters, followed by Rivers and Delta. The larger absolute values of monthly parameters arise from the different temporal aggregation and rainfall units represented by monthly totals. They should not be interpreted as evidence of greater statistical uncertainty without considering their relative magnitudes and posterior intervals.

The absence of visually apparent trends or persistent chain separation supports the numerical stability of the sampling process. Confirmation of convergence, however, requires the associated R-hat, effective sample size, and divergence diagnostics.

Figure 10 presents the marginal posterior probability distributions of the Bayesian Gumbel location (μ) and scale (β) parameters estimated for annual maximum daily rainfall in Bayelsa, Rivers, and Delta States over the 41-year study period (1983–2023).

The posterior distributions provide information on the central estimates, variability, and uncertainty associated with the model parameters. The location parameter (μ) determines the position of the fitted extreme-rainfall distribution, while the scale parameter (β) describes its dispersion. Higher location parameters generally indicate distributions shifted toward greater rainfall intensities, whereas larger scale parameters reflect greater variability in extreme-rainfall magnitudes.

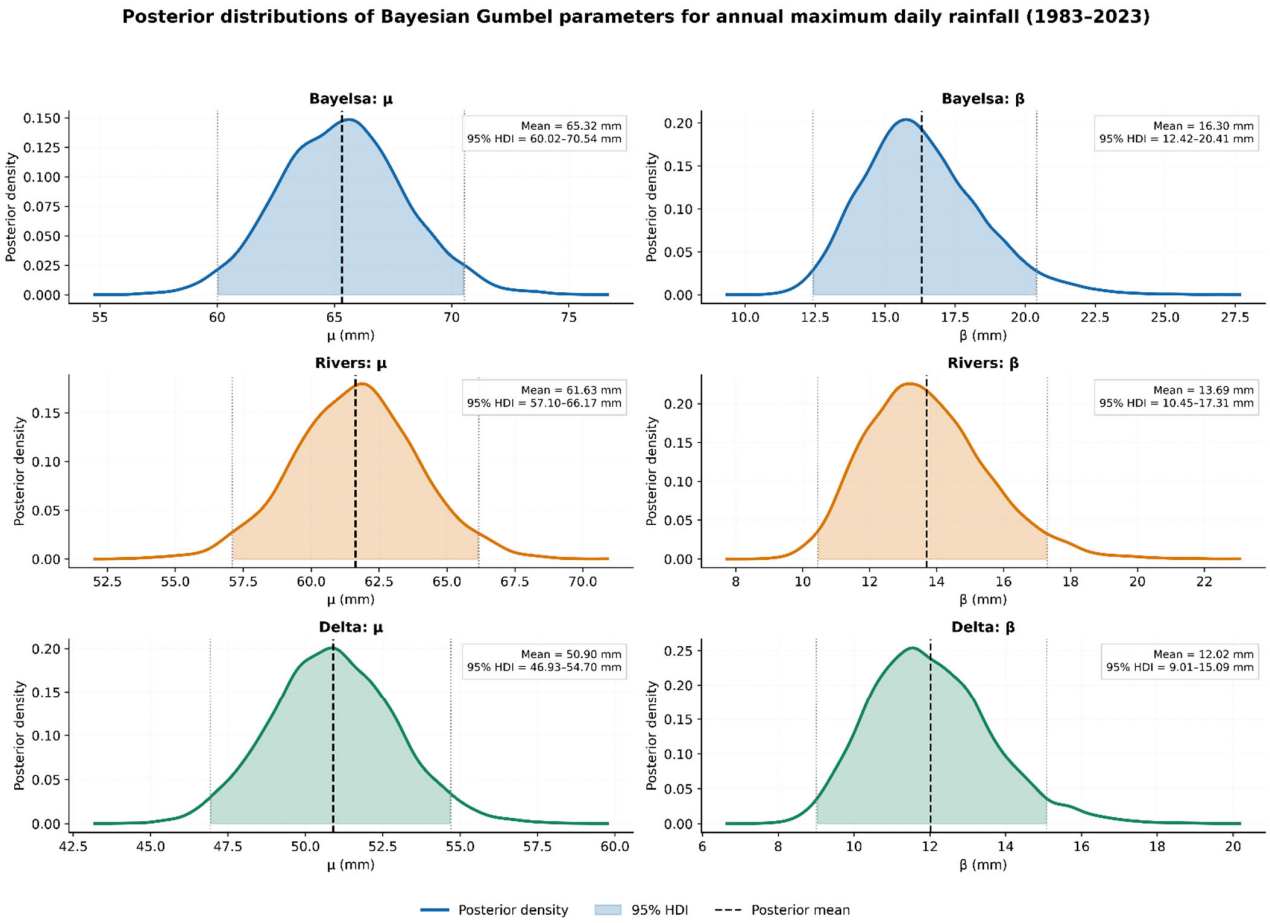


Figure 10. Posterior distributions of Bayesian Gumbel parameters for annual maximum daily rainfall.

The posterior distributions are predominantly unimodal, with well-defined peaks concentrated around their respective posterior means. The dashed vertical lines represent the posterior mean estimates, while the shaded regions indicate the 95% highest-density intervals (HDIs). These intervals represent the most densely concentrated regions containing 95% of the posterior probability for each parameter. The relatively concentrated distributions indicate useful information in the observed annual rainfall maxima for estimating the Gumbel parameters, although uncertainty remains, particularly for the scale parameters.

Bayelsa State exhibits the highest posterior mean location parameter among the three states, estimated at 65.32 mm, with a 95% HDI ranging from 60.02 to 70.54 mm. Its corresponding scale parameter has a posterior mean of 16.30 mm, with a 95% HDI of 12.42–20.41 mm. These estimates indicate that the fitted annual maximum daily rainfall distribution for Bayelsa is positioned toward higher rainfall magnitudes and exhibits greater dispersion than the corresponding distributions for Rivers and Delta States. The relatively high scale parameter suggests considerable interannual variability in annual daily rainfall maxima. This variability is relevant to extreme-rainfall risk assessment because a more dispersed Gumbel distribution assigns greater probability to very high rainfall amounts when other distributional characteristics are comparable. Nevertheless, the uncertainty associated with the scale parameter indicates that the magnitude of this dispersion is not precisely determined.

Rivers State records a posterior mean location parameter of 61.63 mm, with a 95% HDI of 57.10–66.17 mm. Its scale parameter has a posterior mean of 13.69 mm and a 95% HDI of 10.45–17.31 mm. The estimated location parameter is lower than that of Bayelsa but higher than that of Delta, indicating an intermediate position in the fitted distributions of annual maximum daily rainfall. Similarly, the scale parameter suggests less dispersion than Bayelsa but slightly greater dispersion than Delta. The posterior distribution of the location parameter is relatively concentrated, indicating moderate precision in its estimation. However, the uncertainty interval for the scale parameter overlaps with those of Bayelsa and Delta, suggesting that differences in rainfall dispersion are less clearly established than the ordering of posterior means suggests.

Delta State exhibits the lowest posterior mean location parameter, estimated at 50.90 mm, with a 95% HDI ranging from 46.93 to 54.70 mm. The posterior mean scale parameter is 12.02 mm, with a 95% HDI of 9.01–15.09 mm. The result indicate that the fitted distribution of annual maximum daily rainfall in Delta is positioned toward lower rainfall magnitudes relative to Bayelsa and Rivers. Its lower scale parameter also suggests a narrower fitted distribution and comparatively smaller variability in annual daily rainfall maxima. However, the right-skewed characteristics of the Gumbel distribution indicate that unusually high daily rainfall events remain possible.

The interpretation of these differences requires consideration of posterior uncertainty. The 95% HDIs for the location parameters of Bayelsa and Rivers overlap, while the corresponding intervals for Rivers and Delta are separated. The location intervals for Bayelsa and Delta are also clearly separated. In contrast, the 95% HDIs for the scale parameters overlap across all three states. This pattern suggests stronger evidence of differences in the location parameters between Delta and the other states than of differences in the scale parameters. Nevertheless, overlapping or non-overlapping marginal HDIs do not provide a complete Bayesian assessment of pairwise differences. More rigorous comparisons require direct estimation of posterior differences and their associated probabilities using the MCMC samples.

This outcome emphasizes the importance of adopting state-specific extreme-value models rather than assuming identical extreme-rainfall characteristics throughout the Niger Delta. Differences in the estimated location and dispersion parameters indicate that a single regional parameterization might obscure important spatial variations in rainfall behaviour. State-specific parameter estimates therefore provide a more appropriate basis for evaluating extreme-rainfall distributions and developing location-sensitive assessments of hydrological hazards as shown in Figure 11.

Similarly, Figure 11 presents the marginal posterior probability distributions of the Bayesian Gumbel location (μ) and scale (β) parameters estimated for annual maximum monthly rainfall in Bayelsa, Rivers, and Delta States over the 41-year study period (1983–2023). The posterior distributions provide quantitative information on the estimated characteristics of extreme monthly rainfall, including the central parameter estimates, dispersion, and associated uncertainty. The location parameter represents the position of the fitted extreme-rainfall distribution, while the scale parameter describes its variability and spread. Higher location parameters generally indicate distributions shifted toward greater monthly rainfall magnitudes, whereas larger scale parameters reflect greater dispersion in annual maximum monthly rainfall.

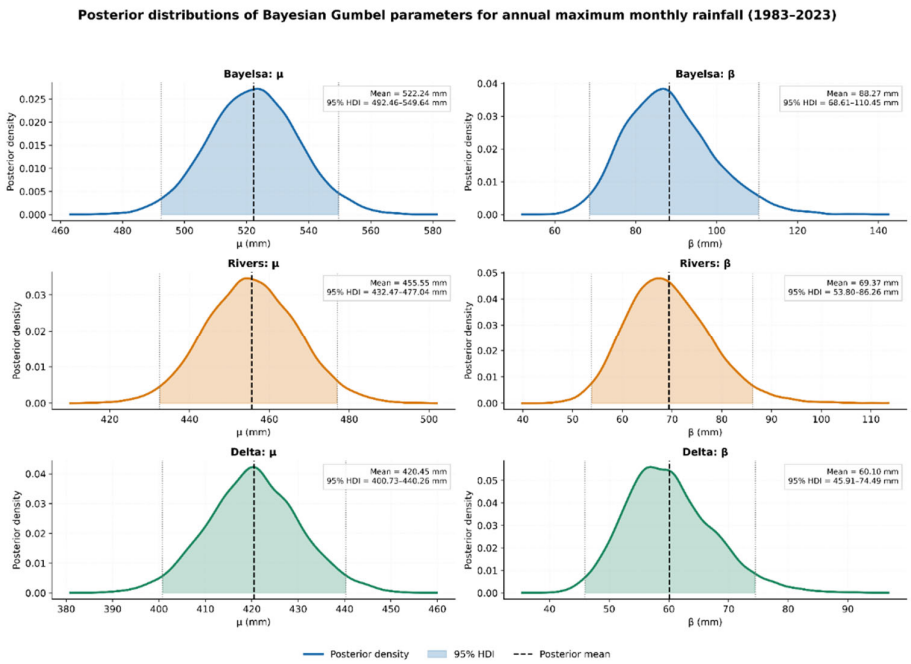


Figure 11. Posterior distributions of Bayesian Gumbel parameters for annual maximum monthly rainfall.

The posterior distributions shown in Figure 10 are predominantly unimodal, with well-defined peaks concentrated around their respective posterior means. The dashed vertical lines represent the posterior mean estimates, while the shaded regions indicate the 95% highest-density intervals (HDIs). These intervals identify the most densely concentrated regions containing 95% of the posterior probability for each parameter. The concentration of the posterior distributions indicates that the observed rainfall maxima provide useful information for estimating the Gumbel parameters. Nevertheless, the widths of the uncertainty intervals demonstrate that parameter estimation remains subject to uncertainty, particularly for the scale parameters.

Bayelsa State exhibits the highest posterior mean location parameter among the three states, estimated at 522.24 mm, with a 95% HDI ranging from 492.46 to 549.64 mm. Its corresponding scale parameter has a posterior mean of 88.27 mm, with a 95% HDI of 68.61–110.45 mm. These estimates indicate that the fitted annual maximum monthly rainfall distribution for Bayelsa is positioned toward higher rainfall magnitudes and exhibits greater dispersion than the corresponding distributions for Rivers and Delta States. The relatively high location parameter suggests that the fitted distribution of annual monthly rainfall maxima is centred at greater rainfall amounts, while the larger scale parameter indicates substantial variability in the magnitude of extreme monthly rainfall events.

The comparatively broad posterior distribution of the scale parameter in Bayelsa reflects uncertainty in the estimated variability of monthly rainfall extremes. This uncertainty is particularly relevant when evaluating rare rainfall events because the scale parameter influences the upper-tail behaviour of the Gumbel distribution and the estimated magnitude of rainfall associated with longer return periods. The combination of a high location parameter and a relatively large scale parameter suggests that Bayelsa has the highest fitted monthly extreme-rainfall magnitudes among the three states, particularly for sufficiently long return periods. However, the strength of this difference requires further evaluation through posterior return-level comparisons. Rivers State records a posterior mean location parameter of 455.55 mm, with a 95% HDI ranging from

432.47 to 477.04 mm. The corresponding scale parameter has a posterior mean of 69.37 mm, with a 95% HDI of 53.80–86.26 mm. These estimates are lower than those obtained for Bayelsa but higher than those of Delta, indicating an intermediate position in the fitted distributions of annual maximum monthly rainfall.

The posterior distribution of the location parameter for Rivers is relatively concentrated around its mean, suggesting moderate precision in the estimated position of the monthly extreme-rainfall distribution. The scale parameter exhibits a broader uncertainty interval, indicating greater uncertainty in the estimated dispersion of extreme monthly rainfall. The lower scale estimate relative to Bayelsa suggests a narrower fitted distribution, although the overlapping uncertainty intervals indicate that the magnitude of the difference in dispersion is not firmly established. The results for Rivers State suggest that its annual maximum monthly rainfall characteristics differ from those of Bayelsa and Delta, particularly in the estimated location of the distribution. The intermediate parameter estimates indicate that Rivers occupies a position between the higher fitted monthly rainfall extremes in Bayelsa and the lower fitted magnitudes in Delta. Nevertheless, this ordering reflects the posterior mean estimates and should not be interpreted as definitive evidence of all pairwise differences without formal posterior comparisons.

Delta State exhibits the lowest posterior mean location parameter, estimated at 420.45 mm, with a 95% HDI ranging from 400.73 to 440.26 mm. Its corresponding scale parameter has a posterior mean of 60.10 mm, with a 95% HDI of 45.91–74.49 mm.

A comparison of the posterior mean estimates reveals a consistent spatial pattern in the fitted Gumbel parameters. Bayelsa records the highest location and scale estimates, followed by Rivers and Delta. The posterior mean location parameter for Bayelsa exceeds that of Rivers by 66.69 mm and Delta by 101.79 mm, while Rivers exceeds Delta by 35.10 mm. Similarly, the posterior mean scale parameter for Bayelsa exceeds that of Rivers by 18.90 mm and Delta by 28.17 mm, while Rivers exceeds Delta by 9.27 mm. These differences indicate spatial heterogeneity in the fitted position and dispersion of annual maximum monthly rainfall distributions across the three states. The larger differences in location parameters suggest that the states experience distinct characteristic magnitudes of annual monthly rainfall maxima. Differences in scale parameters further indicate variations in the dispersion of extreme monthly rainfall, although their statistical interpretation requires consideration of posterior uncertainty.

The 95% HDIs provide additional information regarding the strength of these differences. The location-parameter interval for Bayelsa is separated from the corresponding intervals for Rivers and Delta, indicating comparatively strong evidence of differences in the fitted location parameters. However, the location-parameter intervals for Rivers and Delta overlap slightly, suggesting less definitive separation between these states. In contrast, the uncertainty intervals for the scale parameters overlap across all three states, indicating that differences in dispersion are less clearly established. The overlapping scale-parameter intervals emphasize the importance of distinguishing between differences in posterior mean estimates and evidence of statistically credible parameter differences. Although Bayelsa records the highest estimated scale parameter, the posterior uncertainty does not independently establish that its rainfall dispersion exceeds that of Rivers and Delta with a specified level of posterior probability. More rigorous assessment requires direct comparison of posterior parameter differences using the MCMC samples.

Consequently, uncertainty in both parameters contributes to uncertainty in estimated rainfall return levels.

The result also demonstrates the importance of accounting for spatial heterogeneity when modelling extreme monthly rainfall in the Niger Delta. Applying a single regional

Gumbel distribution to all three states might conceal differences in the location and dispersion of rainfall extremes. State-specific Bayesian parameter estimates therefore provide a more appropriate statistical foundation for comparing extreme-rainfall characteristics and assessing differences in rainfall-related hazards. Nevertheless, the estimated Gumbel parameters represent rainfall characteristics rather than direct measurements of flood frequency, flood depth, or infrastructure vulnerability.

Furthermore, the Bayesian approach provides an explicit representation of uncertainty in the estimated parameters. This is particularly important when analyzing annual rainfall maxima over a limited observational period because estimates of rare events depend on both the available observations and the assumed extreme-value distribution. The posterior distributions therefore provide a foundation for uncertainty-aware return-level estimation and subsequent assessment of rainfall hazards across the three states.

3.3. Peaks-Over-Threshold Generalized Pareto Distribution Analysis and Declustering

The Peaks-Over-Threshold (POT) approach was employed to investigate the statistical characteristics of extreme daily rainfall in Bayelsa, Rivers, and Delta States during 1983–2023. The analysis used the Generalized Pareto Distribution (GPD) to characterize rainfall magnitudes exceeding selected thresholds. Unlike annual block-maxima methods, the POT framework incorporates multiple extreme-rainfall observations within individual years, providing additional information on rainfall extremes and their occurrence frequencies. State-specific empirical rainfall thresholds were determined from the daily CHIRPS rainfall series. The 95th-percentile threshold was selected for the principal POT analysis, while additional thresholds corresponding to the 90th, 92.5th, 97.5th, and 99th percentiles were evaluated to assess parameter sensitivity. A three-day run-length declustering procedure was subsequently applied to reduce temporal dependence among consecutive rainfall exceedances.

At the 95th percentile, the thresholds were 31.65 mm day^{-1} for Bayelsa, 27.43 mm day^{-1} for Rivers, and 25.17 mm day^{-1} for Delta. Each state recorded 749 raw exceedances. Following declustering, 470 events were retained in Bayelsa, 515 in Rivers, and 494 in Delta, corresponding to reductions of 37.2%, 31.2%, and 34.0%, respectively. These reductions indicate that a substantial proportion of daily threshold exceedances occurred within temporally clustered rainfall episodes. The resulting declustered event rates were approximately 11.46, 12.56, and 12.05 events per year for Bayelsa, Rivers, and Delta, respectively.

The final GPD models were fitted to the declustered event maxima. Bayelsa recorded a shape parameter of 0.0182 and scale parameter of 13.71 mm, while Rivers recorded corresponding values of 0.0232 and 12.47 mm. Delta exhibited a slightly negative shape parameter of −0.0194 and a scale parameter of 10.84 mm. These shape estimates are close to zero, suggesting fitted upper-tail characteristics approaching the exponential limiting case. However, their uncertainty must be quantified before making definitive statements about tail classification.

Table 5 presents the sensitivity of the fitted GPD shape and scale parameters to changes in the selected rainfall threshold before declustering. The results demonstrate variations in threshold magnitudes, exceedance counts, and fitted distribution parameters across the three states.

Table 5. POT-sensitivity results before declustering.

State	Percentile	Threshold_mm_Day	Raw_Exceedances	Shape_xi	Scale_beta_mm
Bayelsa	90	23.18646	1498	0.016885	11.85612
Bayelsa	92.5	26.7123	1124	0.029194	11.63638
Bayelsa	95	31.64885	749	0.047683	11.36032
Bayelsa	97.5	39.76647	375	0.080587	11.13757
Bayelsa	99	50.76333	150	0.125026	11.05667
Rivers	90	20.42082	1498	0.067658	9.894476
Rivers	92.5	23.18078	1124	0.053782	10.35182
Rivers	95	27.42987	749	0.054943	10.56214
Rivers	97.5	34.72697	375	0.069189	10.84314
Rivers	99	45.16117	150	0.074758	11.34982
Delta	90	18.76162	1498	0.003866	9.171174
Delta	92.5	21.48468	1124	0.01648	8.960411
Delta	95	25.16891	749	0.025282	8.882711
Delta	97.5	31.51893	375	0.069941	8.391303
Delta	99	39.75677	150	0.146203	7.91097

In Bayelsa, the rainfall threshold increased from 23.19 mm day^{-1} at the 90th percentile to 50.76 mm day^{-1} at the 99th percentile. Correspondingly, the number of raw exceedances decreased from 1498 to 150. The estimated GPD shape parameter increased progressively from 0.0169 to 0.1250, while the scale parameter decreased slightly from 11.86 mm to 11.06 mm. This pattern indicates increasing positive tail-shape estimates as the threshold rises, suggesting sensitivity of the estimated upper-tail characteristics to threshold selection.

In Rivers, the threshold increased from 20.42 mm day^{-1} at the 90th percentile to 45.16 mm day^{-1} at the 99th percentile. The estimated shape parameter varied between 0.0538 and 0.0748, showing comparatively limited variation across the evaluated thresholds. The scale parameter increased from 9.89 mm to 11.35 mm. These results suggest that the fitted shape parameter is relatively stable across the candidate thresholds compared with the patterns observed in Bayelsa and Delta.

Delta recorded thresholds ranging from 18.76 mm day^{-1} at the 90th percentile to 39.76 mm day^{-1} at the 99th percentile. The estimated shape parameter increased from 0.0039 to 0.1462, while the scale parameter decreased from 9.17 mm to 7.91 mm. The pronounced increase in the shape parameter at higher thresholds indicates sensitivity of the fitted upper-tail characteristics to the number and magnitude of retained observations.

Table 6 presents the estimated daily rainfall return levels derived from the state-specific declustered POT-GPD models for return periods of 2, 5, 10, 25, 50, and 100 years. The return-level calculations incorporate the fitted GPD shape and scale parameters, the selected rainfall thresholds, and the declustered event-occurrence rates. Bayelsa records the highest estimated rainfall return levels across all evaluated return periods. Its 2-year return level is 75.85 mm day^{-1}, increasing to 89.26 mm day^{-1} at 5 years and 99.55 mm day^{-1} at 10 years. For longer return periods, the estimated magnitudes increase to 113.36 mm day^{-1} at 25 years, 123.96 mm day^{-1} at 50 years, and 134.70 mm day^{-1} at 100 years.

Table 6. Estimated rainfall return levels for different return periods using the declustered Peaks-Over-Threshold Generalized Pareto Distribution (POT-GPD) model.

State	Return_period_Years	Threshold_mm_Day	Declustered_Events	Run_Length_Days	Event_Rate_per_Year	Shape_xi	Scale_beta_mm	Return_Level_mm_Day
Bayelsa	2	31.64885	470	3	11.46342	0.018171	13.71211	75.84521
Bayelsa	5	31.64885	470	3	11.46342	0.018171	13.71211	89.25669

			470	3	11.46342	0.018171	13.71211	99.55147
Bayelsa	10	31.64885	470	3	11.46342	0.018171	13.71211	113.361
Bayelsa	25	31.64885	470	3	11.46342	0.018171	13.71211	123.9612
Bayelsa	50	31.64885	470	3	11.46342	0.018171	13.71211	134.6959
Bayelsa	100	31.64885	515	3	12.56098	0.023153	12.47332	69.17934
Rivers	2	27.42987	515	3	12.56098	0.023153	12.47332	81.6258
Rivers	5	27.42987	515	3	12.56098	0.023153	12.47332	91.21818
Rivers	10	27.42987	515	3	12.56098	0.023153	12.47332	104.1372
Rivers	25	27.42987	515	3	12.56098	0.023153	12.47332	114.0938
Rivers	50	27.42987	515	3	12.56098	0.023153	12.47332	124.2114
Rivers	100	27.42987	494	3	12.04878	−0.01938	10.83556	58.60733
Delta	2	25.16891	494	3	12.04878	−0.01938	10.83556	67.85974
Delta	5	25.16891	494	3	12.04878	−0.01938	10.83556	74.75059
Delta	10	25.16891	494	3	12.04878	−0.01938	10.83556	83.7189
Delta	25	25.16891	494	3	12.04878	−0.01938	10.83556	90.39816
Delta	50	25.16891	494	3	12.04878	−0.01938	10.83556	96.9883
Delta	100	25.16891	494	3	12.04878	−0.01938	10.83556	96.9883

Rivers exhibits intermediate return-level estimates, increasing from 69.18 mm day^{-1} for the 2-year return period to 81.63 mm day^{-1} at 5 years and 91.22 mm day^{-1} at 10 years. The corresponding 25-year, 50-year, and 100-year return levels are 104.14, 114.09, and 124.21 mm day^{-1}, respectively. Delta records the lowest estimated return levels, with a 2-year value of 58.61 mm day^{-1}, increasing to 67.86 mm day^{-1} at 5 years and 74.75 mm day^{-1} at 10 years. The 25-year, 50-year, and 100-year return levels are estimated at 83.72, 90.40, and 96.99 mm day^{-1}, respectively. At the 100-year return period, Bayelsa exceeds Rivers by approximately 10.48 mm day^{-1} and Delta by 37.71 mm day^{-1}. Rivers exceeds Delta by approximately 27.22 mm day^{-1}. The consistent ordering of the return-level estimates indicates that Bayelsa exhibits the highest fitted extreme daily rainfall magnitudes, followed by Rivers and Delta. This pattern is consistent with the differences in their selected thresholds and fitted GPD parameters.

The estimated return levels increase with return period, reflecting the progressively greater rainfall magnitudes associated with rarer events. However, the estimates represent expected exceedance frequencies under the stationary POT-GPD model and do not imply that events occur at regular intervals. The 100-year return levels require particular caution because the observational record covers only 41 years. These estimates involve extrapolation beyond the observed record length, and their reliability depends on the fitted upper-tail distribution, threshold adequacy, temporal dependence assumptions, and parameter uncertainty. The reported point estimates do not include confidence intervals. The apparent differences among states should be interpreted descriptively until uncertainty in the return levels has been quantified.

Consequently, Figure 12 provides a graphical assessment of the shape-parameter stability across the five candidate thresholds. The Bayelsa panel shows a progressive increase in the shape parameter, particularly beyond the 95th percentile. Rivers exhibits a comparatively stable pattern, with modest fluctuations around values between approximately 0.05 and 0.08. Delta displays a substantial increase at the highest thresholds, particularly between the 97.5th and 99th percentiles.

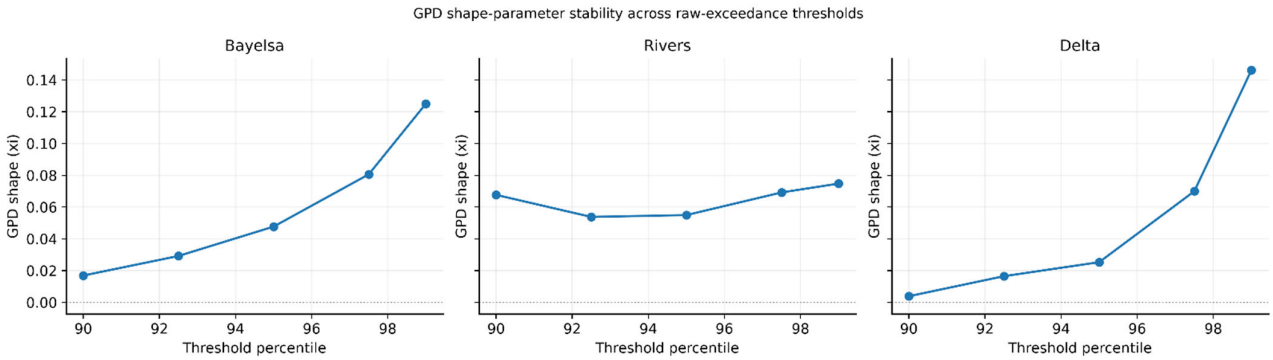


Figure 12. GPD shape-parameter stability across candidate thresholds.

The contrasting patterns demonstrate differences in threshold sensitivity among the three states. Rivers exhibits the greatest apparent shape-parameter stability, while Bayelsa and Delta display more pronounced increases at higher thresholds. The positive shape estimates across the raw-exceedance threshold analyses indicate fitted heavy-tailed GPD distributions. However, the magnitude and statistical significance of these estimates remain uncertain because confidence intervals are not presented. Furthermore, the shape parameters obtained before declustering differ from those estimated using the declustered event maxima.

The 95th-percentile threshold provides a common percentile-based selection criterion across the states while retaining 749 exceedances per state. Nevertheless, the observed parameter variation, particularly in Bayelsa and Delta, indicates that threshold adequacy requires additional assessment. Mean residual life diagnostics, threshold-adjusted scale stability, and parameter confidence intervals would strengthen the threshold-selection justification.

Figure 13 presents the quantile–quantile (Q-Q) diagnostics for the declustered POT-GPD models fitted to rainfall excesses above the selected thresholds. The horizontal axes represent theoretical GPD excess quantiles, while the vertical axes represent observed excess quantiles. The diagonal reference lines indicate perfect agreement between the observed and theoretical quantiles.

For Bayelsa, most of the plotted observations lie close to the diagonal reference line, particularly at low and intermediate excess magnitudes. This indicates generally satisfactory agreement between the fitted GPD model and the empirical distribution of declustered rainfall excesses. However, deviations occur in the upper quantiles, where some observed excesses exceed their theoretical counterparts, while the largest plotted observation falls below its corresponding theoretical quantile. In Rivers, the Q-Q plot also demonstrates close agreement across much of the distribution. Moderate departures occur among the larger excess magnitudes, including observations positioned above and below the reference line. These deviations indicate some differences between the fitted GPD upper tail and the observed extreme-rainfall excesses

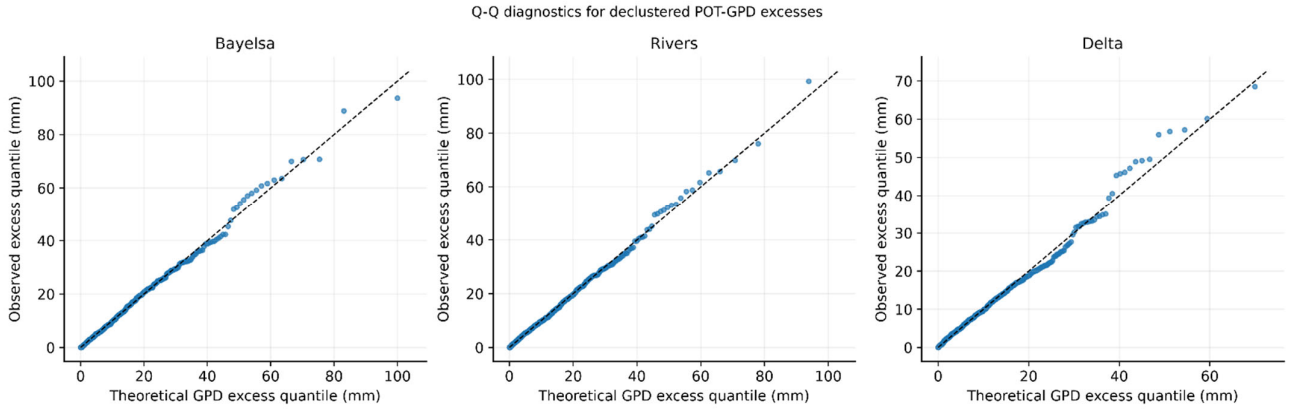


Figure 13. Q-Q diagnostic for the declustered POT/GPD model.

Delta exhibits close agreement at lower excess magnitudes, but more pronounced departures are visible in portions of the upper distribution. Several larger observed excesses exceed their theoretical quantiles, indicating that the fitted model underestimates some observed upper-tail magnitudes. The largest observations nevertheless remain relatively close to the reference line. Collectively, the Q-Q diagnostics indicate that the declustered GPD models reproduce much of the observed excess-rainfall distribution across the three states. However, departures in the upper quantiles demonstrate that the fitted distributions do not perfectly represent the most extreme observations. These differences are particularly relevant for long-return-period rainfall estimation.

The corresponding probability–probability (P-P) diagnostics are presented in Figure 14. The plots compare empirical cumulative probabilities with cumulative probabilities estimated from the fitted GPD models. In Bayelsa, the plotted probabilities closely follow the diagonal reference line across nearly the entire distribution, indicating strong agreement between empirical and fitted cumulative probabilities. Minor deviations are visible in selected probability ranges, but no pronounced systematic departure is apparent. Rivers also exhibits close alignment with the diagonal, although modest deviations occur in the lower-middle and intermediate probability ranges.

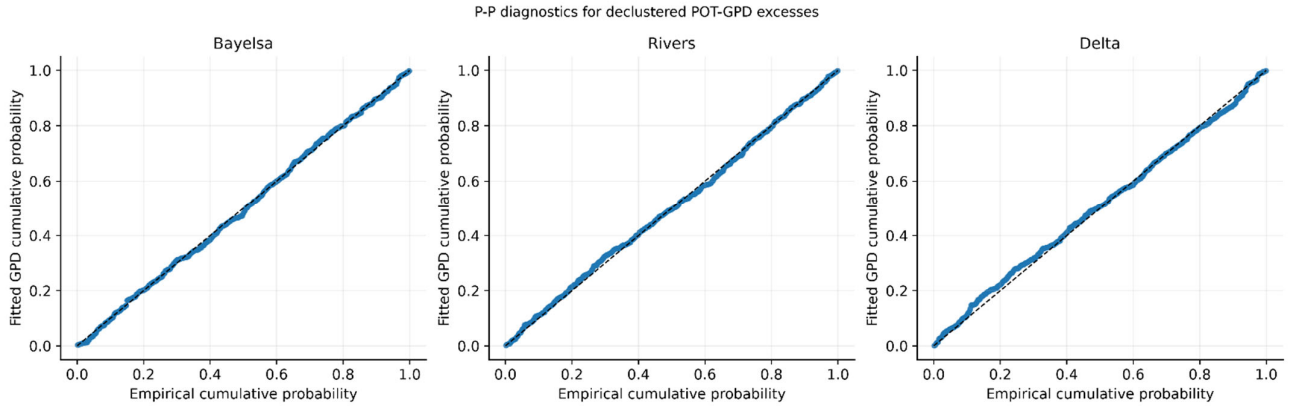


Figure 14. P-P diagnostic for the declustered POT/GPD model.

The fitted probabilities remain broadly consistent with the empirical distribution. Delta displays generally satisfactory agreement, with somewhat more noticeable deviations in the lower-middle probability range. Nevertheless, most observations remain close to the diagonal reference line, indicating reasonable representation of the overall cumulative distribution.

The P-P diagnostics support the general adequacy of the fitted GPD models for describing the bulk of the declustered exceedance distributions. However, close agreement in P-P plots does not guarantee accurate estimation of the most extreme-rainfall quantiles because the upper tail occupies a relatively small portion of the cumulative probability range. The combined interpretation of Figures 13 and 14 therefore indicates broadly satisfactory distributional agreement, accompanied by localized upper-tail deviations.

The daily rainfall time series and raw POT exceedances above the state-specific empirical 95th-percentile thresholds for Bayelsa, Rivers, and Delta States during 1983–2023 is presented in Figure 15. The continuous lines represent daily rainfall, the highlighted points identify threshold exceedances, and the horizontal dashed lines indicate the selected rainfall thresholds. The Bayelsa rainfall series exhibits the highest threshold, at 31.65 mm day^{-1}. The figure shows numerous exceedances distributed throughout the study period, including several individual rainfall events exceeding 100 mm day^{-1}. The largest plotted daily rainfall magnitudes approach approximately 125 mm. The distribution of exceedances also indicates episodes of temporally concentrated heavy rainfall, supporting the application of declustering.

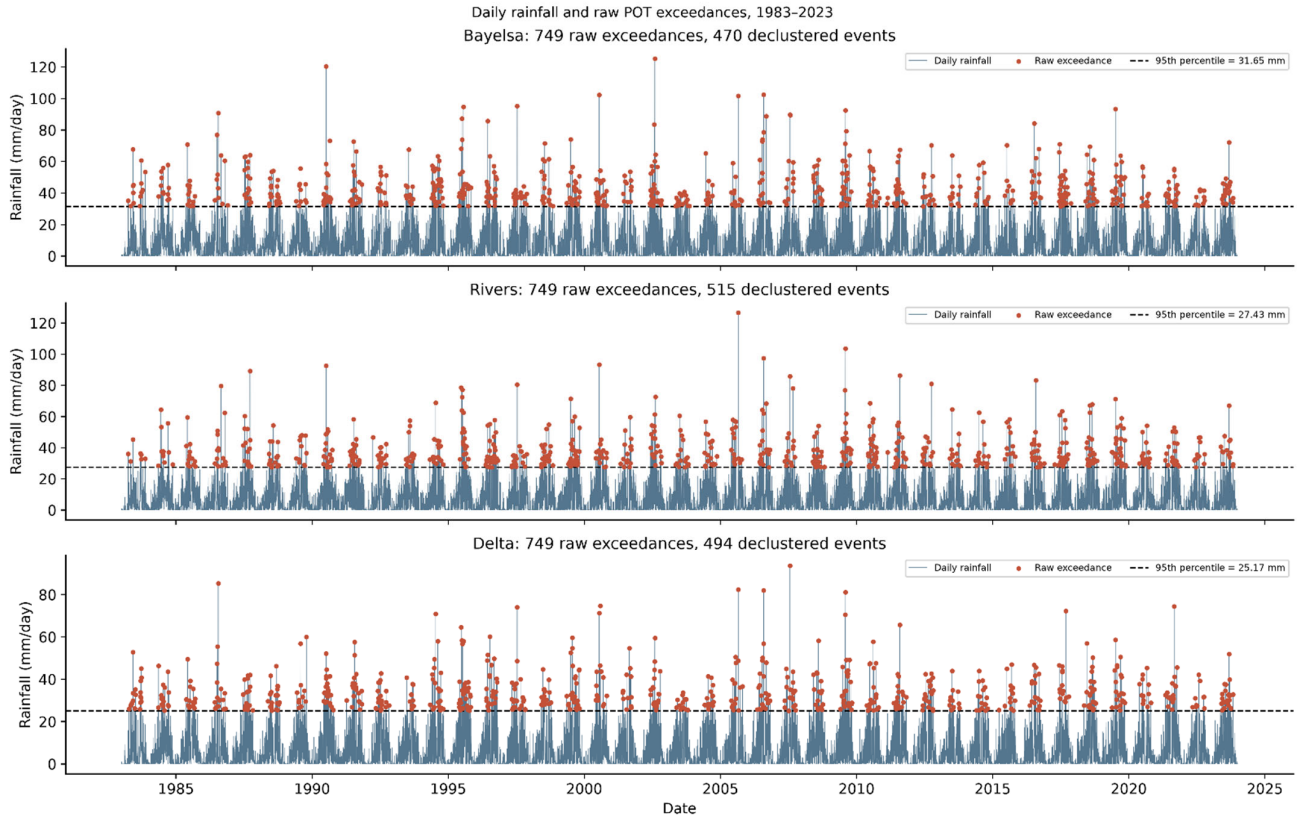


Figure 15. Daily rainfall series and raw POT exceedances above the empirical 95th-percentile threshold (19.58 mm/day), 1983–2023.

Bayelsa recorded 749 raw exceedances, reduced to 470 approximately independent events following the three-day declustering procedure. This represents a reduction of 279 observations, equivalent to approximately 37.2% of the original exceedance count. The relatively large reduction indicates substantial temporal clustering of rainfall exceedances. Rivers State exhibits a threshold of 27.43 mm day^{-1}, with extreme-rainfall observations occurring throughout the study period. Several daily rainfall events exceed 80 mm, while

the largest plotted observation reaches approximately 125 mm. The exceedances exhibit temporal clustering, although the reduction following declustering is smaller than in Bayelsa.

The number of raw exceedances in Rivers decreased from 749 to 515 independent-event maxima, representing a reduction of approximately 31.2%. The resulting event-occurrence rate of 12.56 events per year is the highest among the three states. This indicates that Rivers retained the greatest number of approximately independent threshold-exceeding events under the adopted state-specific thresholds and declustering procedure. Delta State exhibits the lowest 95th-percentile threshold, at 25.17 mm day^{-1}. The daily rainfall series contains numerous exceedances, with the largest plotted rainfall magnitudes approaching approximately 95 mm. The occurrence of consecutive exceedances indicates temporal clustering of heavy rainfall events. Following declustering, the 749 raw exceedances in Delta were reduced to 494 approximately independent events, representing a reduction of approximately 34.0%. The corresponding event rate was 12.05 events per year. The comparison demonstrates that Bayelsa has the highest absolute 95th-percentile rainfall threshold, followed by Rivers and Delta. However, the equal number of raw exceedances results from the percentile-based threshold selection and equal record lengths, rather than identical absolute frequencies of rainfall above a common fixed threshold.

The differences in declustered event counts indicate variation in the temporal organization of rainfall exceedances. Bayelsa exhibits the greatest reduction, followed by Delta and Rivers. These findings suggest differences in the persistence or clustering of heavy rainfall episodes across the states, although a detailed assessment of rainfall-event duration would require additional event-based analysis. The distribution of exceedances across the study period also indicates that extreme rainfall occurred in multiple years rather than being restricted to a single short interval. However, the figure alone does not establish statistically significant temporal trends in extreme-rainfall frequency or intensity.

3.4. Classical Gumbel Extreme Value Theory and Log-Pearson Type III Distributions

Classical extreme-value frequency analysis was conducted using the Gumbel and Log-Pearson Type III (LP3) probability distributions to estimate the magnitude of extreme-rainfall events across Bayelsa, Rivers, and Delta States during 1983–2023. Annual maximum daily rainfall (AMAX-D) and annual maximum monthly rainfall (AMAX-M) were extracted separately for each state, producing 41 annual observations for each rainfall accumulation period. The two probability distributions were fitted independently to each series, and comparisons were restricted to the same state and temporal accumulation period to ensure statistical consistency.

The Gumbel distribution was fitted using maximum-likelihood estimation, while the LP3 distribution was applied to logarithmically transformed annual maximum rainfall observations. Return levels were estimated for recurrence intervals of 2, 5, 10, 25, 50, and 100 years. Tables 7 and 8 present the Gumbel-based 100-year return levels for annual maximum daily and monthly rainfall, respectively, together with their corresponding 95% bootstrap confidence intervals. The additional return periods were retained in the underlying frequency-analysis outputs.

Table 7. State-specific 100-year return levels for annual maximum daily rainfall (AMAX-D), with reported 95% uncertainty bounds (1983–2023; n = 41 per state).

State	Series	Model	Return_Period_Years	Return_Level_mm	Bootstrap_95_LOWER_mm	Bootstrap_95_Upper_mm	Bootstrap_Valid_Replicates
Bayelsa	Daily	Gumbel	100	136.7145	115.9642	154.089	500
Rivers	Daily	Gumbel	100	121.4132	103.9983	137.9243	500

Delta	Daily	Gumbel	100	103.2596	89.32688	114.9244	500

Table 8. State-specific 100-year return levels for annual maximum monthly rainfall (AMAX-M), with reported 95% uncertainty bounds (1983–2023; n = 41 per state).

State	Series	Model	Return_ Period_Years	Return_Lev el_mm	Bootstrap_95_ LOWER_mm	Bootstrap_95_ Upper_mm	Bootstrap_Valid _Replicates
Bayelsa	Monthly	Gumbel	100	910.9245	830.5632	978.6887	500
Rivers	Monthly	Gumbel	100	760.5215	685.8379	830.5229	500
Delta	Monthly	Gumbel	100	684.2756	624.9838	733.8286	500

3.4.1. Gumbel Return-Level Estimates for Annual Maximum Daily Rainfall

The results presented in Table 7 indicate clear differences in the estimated magnitude of extreme daily rainfall across the three states. Bayelsa recorded the highest Gumbel-based 100-year return level of 136.71 mm, with a 95% bootstrap confidence interval of 115.96–154.09 mm. Rivers recorded a corresponding return level of 121.41 mm, with confidence bounds of 104.00–137.92 mm, while Delta recorded the lowest estimate of 103.26 mm, with confidence bounds of 89.33–114.92 mm. These estimates indicate a consistent ordering of extreme daily rainfall magnitudes, with Bayelsa exhibiting the highest estimated return level, followed by Rivers and Delta. The estimated 100-year daily rainfall magnitude in Bayelsa exceeds the corresponding estimate for Rivers by approximately 12.6% and Delta by approximately 32.4%. Similarly, the estimated return level for Rivers exceeds Delta by approximately 17.6%.

The differences suggest spatial variation in the upper-tail characteristics of annual maximum daily rainfall across the study area. Bayelsa exhibits the greatest estimated extreme daily rainfall magnitude under the fitted Gumbel model, while Delta exhibits the lowest. However, these estimates represent model-based precipitation quantiles rather than observed rainfall amounts associated with an actual 100-year monitoring period. The confidence intervals indicate uncertainty in the estimated return levels arising from the limited observational record and the variability of the annual maxima. The intervals overlap between Bayelsa and Rivers, while those for Rivers and Delta also overlap. Consequently, the numerical differences between the state-specific estimates should not be interpreted as statistically significant without formal comparative uncertainty analysis.

Furthermore, the 100-year return levels were estimated from 41 annual maximum observations. Their interpretation therefore involves extrapolation beyond the observational record and depends on the suitability of the fitted Gumbel distribution, the stability of its estimated parameters, and the assumption of stationary extreme-rainfall behaviour.

3.4.2. Gumbel Return-Level Estimates for Annual Maximum Monthly Rainfall

The annual maximum monthly rainfall results presented in Table 8 demonstrate substantial differences in estimated extreme monthly rainfall magnitudes across the three states. Bayelsa recorded the highest Gumbel-based 100-year return level of 910.92 mm, with a 95% bootstrap confidence interval of 830.56–978.69 mm. Rivers recorded a corresponding return level of 760.52 mm, with confidence bounds of 685.84–830.52 mm, while Delta recorded the lowest estimated return level of 684.28 mm, with confidence bounds of 624.98–733.83 mm.

The estimated 100-year monthly rainfall return level for Bayelsa exceeds that of Rivers by approximately 19.8% and Delta by approximately 33.1%. Rivers also records a higher estimate than Delta, with a difference of approximately 11.1%. These results

indicate a consistent ordering of estimated extreme-rainfall magnitudes across the three states, with Bayelsa exhibiting the highest values under the Gumbel distribution.

The differences in estimated monthly return levels reflect variations in the distribution of annual maximum monthly rainfall across the study area. Unlike daily rainfall extremes, which represent short-duration precipitation intensity, annual maximum monthly rainfall describes the largest accumulated monthly precipitation within each year. The resulting return levels therefore characterize extreme monthly accumulation rather than individual storm intensity.

The confidence intervals further demonstrate uncertainty associated with long-return-period rainfall estimation. The Bayelsa and Rivers intervals are nearly adjacent, whereas the Rivers and Delta intervals overlap. Nevertheless, confidence-interval overlap alone is insufficient to establish the statistical significance or non-significance of differences between state-specific return levels.

The estimated monthly return levels were also interpreted in relation to the model-comparison results presented in Table 8. Although the Gumbel distribution provides a consistent basis for estimating extreme monthly rainfall, LP3 generally demonstrates closer empirical quantile agreement for annual maximum monthly rainfall across the three states. Consequently, the reported Gumbel return levels are based on the selected probability distribution and should not be regarded as model-independent estimates.

3.4.3. Comparative Interpretation of Daily and Monthly Rainfall Extremes

The classical frequency-analysis results reveal consistent geographical differences in estimated extreme-rainfall magnitudes across the three Niger Delta states. Bayelsa records the highest 100-year return levels for both annual maximum daily and annual maximum monthly rainfall, followed by Rivers and Delta.

For annual maximum daily rainfall, the estimated 100-year return levels range from 103.26 mm in Delta to 136.71 mm in Bayelsa. For annual maximum monthly rainfall, the corresponding estimates range from 684.28 mm in Delta to 910.92 mm in Bayelsa. These differences indicate variation in the fitted distributions of annual maximum rainfall across the study area.

However, direct numerical comparison between daily and monthly return levels requires caution because the two series represent different rainfall accumulation periods. A daily return level describes an extreme 24 h accumulation, while a monthly return level represents an extreme monthly accumulation. The larger monthly values therefore do not independently indicate greater rainfall intensity.

The result further illustrates the importance of considering geographical differences, rainfall accumulation periods, model selection, and estimation uncertainty when assessing extreme rainfall in the Niger Delta. Although the Gumbel distribution provides a common framework for comparing state-specific return levels, the complementary LP3 analysis and goodness-of-fit evaluation are necessary to assess the sensitivity of extreme-rainfall estimates to the assumed probability distribution.

Table 7 presents the state-specific 100-year return levels estimated using the Gumbel distribution fitted to annual maximum daily rainfall (AMAX-D) in Bayelsa, Rivers, and Delta States during 1983–2023. Each state-specific model was fitted to 41 annual maximum observations, and uncertainty was quantified using 500 nonparametric bootstrap replicates. Bayelsa records the highest estimated 100-year daily rainfall return level of 136.71 mm, with a 95% bootstrap confidence interval of 115.96–154.09 mm. This indicates that the fitted Gumbel distribution associates a daily rainfall magnitude of approximately 136.71 mm with a 100-year return period under the stationary model assumptions.

Rivers records an estimated 100-year return level of 121.41 mm, with a 95% bootstrap confidence interval of 104.00–137.92 mm. The point estimate is approximately 15.30 mm

lower than Bayelsa, suggesting a lower fitted magnitude of rare daily rainfall extremes. Delta exhibits the lowest estimated 100-year return level of 103.26 mm, with a 95% bootstrap confidence interval of 89.33–114.92 mm. The estimate is approximately 33.45 mm lower than Bayelsa and 18.15 mm lower than Rivers.

The results establish a consistent ordering of estimated daily rainfall extremes, with Bayelsa recording the highest 100-year return level, followed by Rivers and Delta. This pattern is consistent with the spatial differences identified in the fitted Gumbel location and scale parameters. However, the bootstrap confidence intervals overlap between Bayelsa and Rivers and between Rivers and Delta. The confidence intervals for Bayelsa and Delta are separated, indicating a clearer distinction between their estimated extreme-rainfall magnitudes. Nevertheless, formal comparisons of return-level differences are required to establish the statistical strength of these spatial differences.

The relatively wide confidence intervals reflect uncertainty associated with estimating a 100-year event from a 41-year observational record. The results emphasize the importance of incorporating parameter uncertainty into extreme-rainfall assessments rather than relying exclusively on point estimates.

Table 8 presents the estimated 100-year return levels for annual maximum monthly rainfall (AMAX-M) using the Gumbel distribution. The analysis was conducted separately for Bayelsa, Rivers, and Delta States using 41 annual maximum monthly rainfall observations per state. Bayelsa records the highest estimated 100-year monthly rainfall return level of 910.92 mm, with a 95% bootstrap confidence interval of 830.56–978.69 mm. This indicates that the fitted Gumbel model associates a monthly rainfall accumulation of approximately 910.92 mm with a 100-year return period.

Rivers records a 100-year return level of 760.52 mm, with a 95% bootstrap confidence interval of 685.84–830.52 mm. This estimate is approximately 150.40 mm lower than the corresponding value for Bayelsa. Delta exhibits the lowest estimated 100-year monthly rainfall return level of 684.28 mm, with a 95% bootstrap confidence interval of 624.98–733.83 mm. The estimated return level is approximately 226.65 mm lower than Bayelsa and 76.25 mm lower than Rivers.

The results demonstrate substantial spatial differences in the fitted magnitudes of rare monthly rainfall accumulations. Bayelsa consistently exhibits the highest estimated extreme-rainfall magnitude, followed by Rivers and Delta. The bootstrap confidence intervals for Bayelsa and Rivers are nearly adjacent, while those for Rivers and Delta overlap. The intervals for Bayelsa and Delta are clearly separated. These patterns indicate that uncertainty remains important when comparing the estimated monthly rainfall extremes across states.

The monthly return levels are substantially larger in numerical magnitude than the corresponding daily return levels because they represent accumulated rainfall over an entire month rather than a single day. Consequently, daily and monthly return levels should not be interpreted as equivalent rainfall-intensity measures. The estimated monthly return levels are relevant to assessments of prolonged rainfall accumulation, catchment wetness, seasonal flooding, and hydrological stress. However, monthly rainfall totals alone do not determine flood occurrence or severity, which also depend on rainfall distribution within the month, antecedent conditions, drainage characteristics, and other hydrological factors.

The confidence intervals demonstrate considerable uncertainty in long-return-period estimation. This uncertainty is particularly important because the 100-year return period extends beyond the 41-year observational record. The findings provide a quantitative basis for evaluating differences in rare monthly rainfall accumulation across the three states. Nevertheless, the Gumbel-based return levels should be interpreted alongside the

model-comparison results, which indicate that the LP3 distribution provides closer Q-Q agreement for monthly rainfall maxima.

3.5. Goodness-of-Fit Tests and Model Performance Evaluation

The goodness-of-fit and model performance evaluation was conducted to assess the suitability of the Gumbel and Log-Pearson Type III (LP3) probability distributions for modelling annual maximum daily rainfall (AMAX-D) and annual maximum monthly rainfall (AMAX-M) across Bayelsa, Rivers, and Delta States during the 1983–2023 study period. For each state and rainfall accumulation period, both distributions were fitted to the same 41 annual maximum observations, providing a consistent basis for comparing their statistical performance. Model evaluation was undertaken using the Akaike Information Criterion (AIC), Bayesian Information Criterion (BIC), quantile–quantile root mean square error (Q-Q RMSE), and quantile–quantile mean absolute error (Q-Q MAE), as presented in Table 9.

Table 9. State-specific Gumbel and LP3 model-comparison diagnostics for annual maximum daily and monthly rainfall (n = 41 per state and accumulation period).

State	Series	Index	Model	AIC	BIC	Q-Q RMSE (mm)	Q-Q MAE (mm)
Bayelsa	Daily	AMAX_D	Gumbel	357.6324	361.0595	3.203487	2.49
Bayelsa	Daily	AMAX_D	LP3	359.6263	364.767	3.115594	2.47
Bayelsa	Monthly	AMAX_M	Gumbel	492.7161	496.1432	29.20807	19.32
Bayelsa	Monthly	AMAX_M	LP3	490.0215	495.1623	11.30025	9.94
Rivers	Daily	AMAX_D	Gumbel	345.4099	348.837	2.17894	1.64
Rivers	Daily	AMAX_D	LP3	346.5842	351.7249	1.996004	1.45
Rivers	Monthly	AMAX_M	Gumbel	473.4489	476.8761	17.30311	12.94
Rivers	Monthly	AMAX_M	LP3	473.0941	478.2349	11.16088	9.00
Delta	Daily	AMAX_D	Gumbel	333.9122	337.3394	2.614178	1.98
Delta	Daily	AMAX_D	LP3	335.6624	340.8031	2.921152	2.06
Delta	Monthly	AMAX_M	Gumbel	462.0012	465.4283	15.02264	11.28
Delta	Monthly	AMAX_M	LP3	461.4984	466.6391	7.309507	6.26

The AIC and BIC assess the relative performance of competing probability distributions by considering model likelihood and complexity, with lower values indicating a more favourable balance between goodness of fit and the number of estimated parameters. The Q-Q RMSE and MAE quantify deviations between observed rainfall quantiles and corresponding theoretical quantiles estimated from the fitted distributions. Lower Q-Q errors indicate closer agreement with the empirical rainfall distribution. These measures provide complementary information because likelihood-based model selection and quantile-fitting accuracy do not necessarily identify the same preferred distribution.

For annual maximum daily rainfall in Bayelsa State, the Gumbel distribution recorded an AIC of 357.6324 and BIC of 361.0595, compared with 359.6263 and 364.7670 for LP3. The lower information criteria favour the Gumbel distribution, indicating a more favourable balance between goodness of fit and model complexity. However, LP3 produced slightly lower Q-Q errors, with an RMSE of 3.1156 mm and MAE of 2.47 mm, compared with 3.2035 mm and 2.49 mm for Gumbel. The relatively small differences in quantile-fitting errors suggest comparable empirical performance for annual maximum daily rainfall, although the information criteria favour the simpler Gumbel formulation. For annual maximum monthly rainfall in Bayelsa, LP3 demonstrated better performance across all four evaluation criteria. The LP3 distribution recorded an AIC of 490.0215 and BIC of 495.1623, compared with 492.7161 and 496.1432 for Gumbel. More pronounced

differences were observed in the Q-Q diagnostics, where LP3 achieved an RMSE of 11.3003 mm and MAE of 9.94 mm, compared with 29.2081 mm and 19.32 mm for Gumbel. The reduction in Q-Q RMSE was approximately 61.3%, while MAE decreased by approximately 48.6%. These results indicate substantially closer agreement between the LP3 theoretical quantiles and the observed annual maximum monthly rainfall distribution in Bayelsa. In Rivers State, the Gumbel distribution also produced lower information criteria for annual maximum daily rainfall. The Gumbel model recorded an AIC of 345.4099 and BIC of 348.8370, compared with 346.5842 and 351.7249 for LP3. However, LP3 achieved a lower Q-Q RMSE of 1.9960 mm and MAE of 1.45 mm, compared with 2.1789 mm and 1.64 mm for Gumbel. These results indicate that LP3 provides slightly closer empirical quantile agreement, while Gumbel remains preferable under the information criteria.

For annual maximum monthly rainfall in Rivers, the model-comparison results were mixed. LP3 recorded a marginally lower AIC of 473.0941, compared with 473.4489 for Gumbel. Conversely, Gumbel produced a lower BIC of 476.8761, compared with 478.2349 for LP3. The small differences between the information criteria indicate limited evidence for a clear model preference based on likelihood and complexity. Nevertheless, LP3 achieved a lower Q-Q RMSE of 11.1609 mm and MAE of 9.00 mm, compared with 17.3031 mm and 12.94 mm for Gumbel. These represent reductions of approximately 35.5% and 30.4%, respectively, indicating improved empirical quantile-fitting performance for the LP3 distribution. For annual maximum daily rainfall in Delta State, the Gumbel distribution demonstrated better performance across all four diagnostic measures. The Gumbel model recorded an AIC of 333.9122 and BIC of 337.3394, compared with 335.6624 and 340.8031 for LP3. Its Q-Q RMSE and MAE were 2.6142 mm and 1.98 mm, respectively, compared with 2.9212 mm and 2.06 mm for LP3.

For annual maximum monthly rainfall in Delta, LP3 recorded a slightly lower AIC of 461.4984, compared with 462.0012 for Gumbel. However, Gumbel produced a lower BIC of 465.4283, compared with 466.6391 for LP3. Despite these mixed information-criterion results, LP3 demonstrated substantially better Q-Q performance, with an RMSE of 7.3095 mm and MAE of 6.26 mm, compared with 15.0226 mm and 11.28 mm for Gumbel. These differences correspond to reductions of approximately 51.3% in RMSE and 44.5% in MAE, indicating closer agreement between LP3 and the observed annual maximum monthly rainfall quantiles. Comparatively, the results reveal a consistent distinction between daily and monthly extreme-rainfall modelling. For annual maximum daily rainfall, Gumbel recorded lower AIC and BIC values across all three states. This indicates that its simpler two-parameter formulation provides a favourable balance between likelihood-based goodness of fit and model complexity. However, LP3 produced slightly smaller Q-Q errors in Bayelsa and Rivers, whereas Gumbel performed better across all four criteria in Delta.

For annual maximum monthly rainfall, LP3 recorded lower AIC values and smaller Q-Q RMSE and MAE values across all three states. The improvement in quantile-fitting accuracy was particularly pronounced in Bayelsa and Delta. Nevertheless, BIC favoured Gumbel in Rivers and Delta, indicating that the additional flexibility of LP3 was not consistently supported after applying the stronger model-complexity penalty associated with BIC.

The graphical Q-Q diagnostics presented in Figure 16 provide additional evidence supporting these findings. For annual maximum daily rainfall, both distributions generally reproduced the observed quantiles with relatively small deviations from the diagonal reference lines. However, the monthly Gumbel models exhibited more pronounced departures, particularly in the upper quantiles. The monthly LP3 models generally demonstrated closer agreement with the observed rainfall distributions,

consistent with their lower Q-Q RMSE and MAE values. Despite these findings, the goodness-of-fit results should not be interpreted as definitive evidence that either distribution is universally superior for estimating rare rainfall events. AIC and BIC provide relative measures of model performance within the fitted dataset, while Q-Q RMSE and MAE quantify differences between observed and theoretical quantiles. Importantly, the reported Q-Q errors represent descriptive in-sample measures rather than independent out-of-sample predictive scores. Consequently, lower Q-Q errors do not necessarily indicate greater predictive accuracy for future extreme-rainfall events.

Furthermore, satisfactory agreement between observed and theoretical quantiles does not guarantee reliable extrapolation to long return periods. Estimation of 50-year and 100-year rainfall magnitudes from a 41-year observational record involves substantial uncertainty associated with the fitted distribution, upper-tail behaviour, parameter estimation, and assumptions of stationarity and independence. The relatively small differences in AIC and BIC for several model comparisons also warrant careful interpretation. Differences of less than approximately two units generally indicate limited separation between competing models under the corresponding information criterion. Consequently, the small information-criterion differences observed for several state-specific comparisons should not be interpreted as strong evidence of model superiority.

The results demonstrate the importance of applying multiple complementary diagnostics when evaluating extreme-value distributions. Although Gumbel provides a parsimonious representation of annual maximum daily rainfall across the three states, LP3 generally achieves closer empirical quantile agreement for annual maximum monthly rainfall. The final selection of a probability distribution for extreme-rainfall return-level estimation should therefore consider the intended application, upper-tail performance, uncertainty intervals, and sensitivity of the estimated return levels to model choice.

Table 9 compares the statistical performance of the Gumbel and Log-Pearson Type III (LP3) distributions fitted to annual maximum daily and monthly rainfall in Bayelsa, Rivers, and Delta States. Model performance was assessed using the Akaike Information Criterion (AIC), Bayesian Information Criterion (BIC), and Q-Q root mean square error (RMSE). For annual maximum daily rainfall in Bayelsa, the Gumbel distribution records an AIC of 357.63 and BIC of 361.06, compared with 359.63 and 364.77 for LP3. The lower information criteria favour Gumbel, while LP3 produces a slightly smaller Q-Q RMSE of 3.12 mm compared with 3.20 mm for Gumbel. These results indicate broadly comparable empirical quantile-fitting performance, with the information criteria favouring the simpler Gumbel model.

For annual maximum monthly rainfall in Bayelsa, LP3 demonstrates better performance under both information criteria and Q-Q RMSE. The LP3 model records an AIC of 490.02, BIC of 495.16, and Q-Q RMSE of 11.30 mm, compared with 492.72, 496.14, and 29.21 mm for Gumbel. The substantial reduction in Q-Q RMSE indicates that LP3 more closely reproduces the observed monthly rainfall quantiles. In Rivers State, the Gumbel distribution records lower AIC and BIC values for annual maximum daily rainfall, with values of 345.41 and 348.84, compared with 346.58 and 351.72 for LP3. However, LP3 produces a slightly lower Q-Q RMSE of 2.00 mm compared with 2.18 mm for Gumbel.

For monthly rainfall in Rivers, LP3 records a slightly lower AIC of 473.09 compared with 473.45 for Gumbel, while Gumbel records a lower BIC of 476.88 compared with 478.23 for LP3. The Q-Q RMSE favours LP3, with an error of 11.16 mm compared with 17.30 mm for Gumbel. These results indicate that model preference depends on the diagnostic criterion. In Delta State, the Gumbel distribution demonstrates better performance across the reported information criteria and Q-Q RMSE for annual maximum daily rainfall. Its AIC, BIC, and Q-Q RMSE are 333.91, 337.34, and 2.61 mm, respectively, compared with 335.66, 340.80, and 2.92 mm for LP3. These findings favour Gumbel for the

daily rainfall series. For annual maximum monthly rainfall in Delta, LP3 records a slightly lower AIC of 461.50 compared with 462.00 for Gumbel, while Gumbel produces a lower BIC of 465.43 compared with 466.64 for LP3. However, LP3 achieves a substantially lower Q-Q RMSE of 7.31 mm compared with 15.02 mm for Gumbel.

Across the three states, Gumbel consistently records lower AIC and BIC values for annual maximum daily rainfall. For monthly rainfall, LP3 records lower AIC values and smaller Q-Q RMSE values in all three states, although BIC favours Gumbel in Rivers and Delta. These results indicate that the relative performance of Gumbel and LP3 depends on the rainfall accumulation period and the selected evaluation criterion. The Gumbel distribution provides a parsimonious representation of annual maximum daily rainfall, while LP3 generally achieves closer empirical quantile agreement for monthly rainfall. However, lower overall Q-Q errors do not necessarily establish superior upper-tail extrapolation. Arising from above, its imperative for rare-event estimation to consider upper-tail diagnostics, uncertainty intervals, and the sensitivity of estimated return levels to the selected distribution.

Similarly, the Q-Q diagnostics for the Gumbel and LP3 distributions fitted to annual maximum daily and monthly rainfall in Bayelsa, Rivers, and Delta States for the entire study period of 1983–2023 is shown in Figure 16. The result consists of twelve panels arranged by state and model. The rows represent Bayelsa, Rivers, and Delta, while the columns correspond to daily Gumbel, daily LP3, monthly Gumbel, and monthly LP3 models. The diagonal dashed lines represent perfect agreement between observed and theoretical rainfall quantiles.

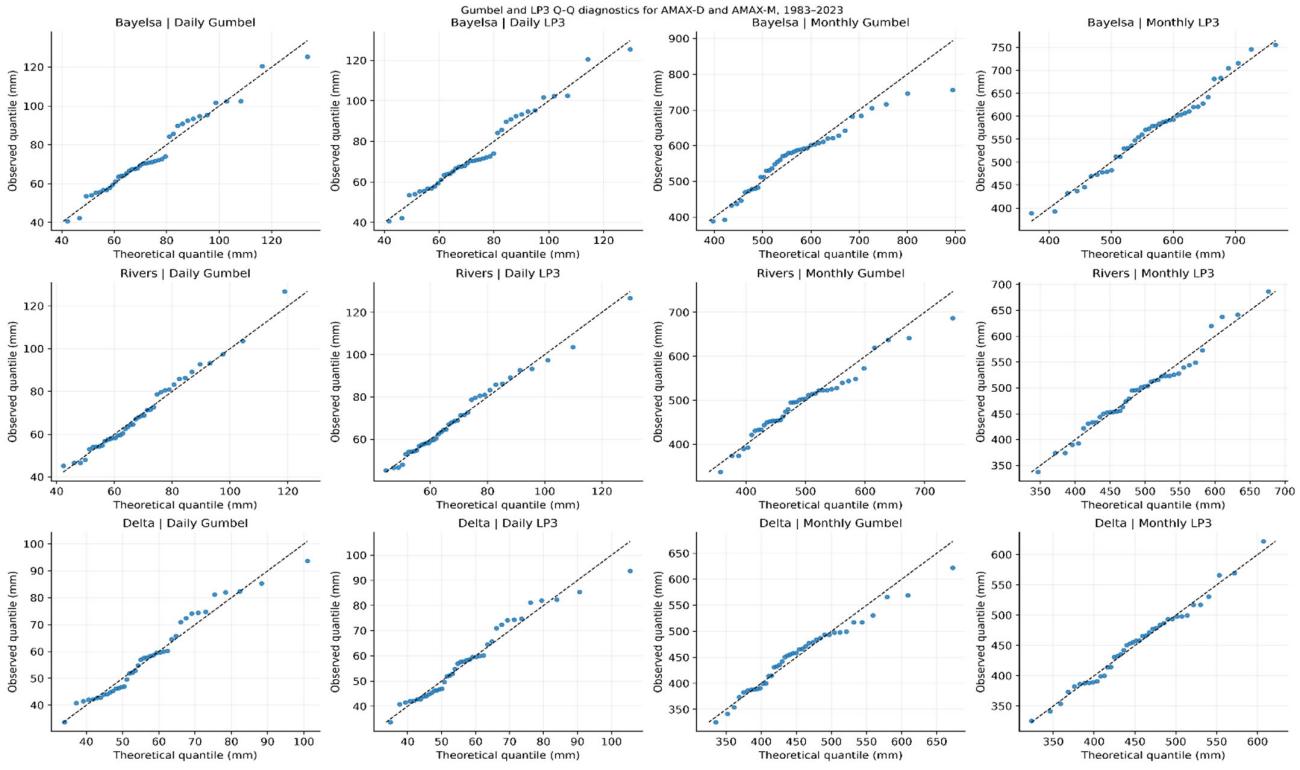


Figure 16. Q-Q diagnostics for Gumbel and LP3 fitted to annual maximum daily (AMAX-D) and monthly (AMAX-M) rainfall in Bayelsa, Rivers, and Delta, 1983–2023. Rows correspond to states; columns to daily Gumbel, daily LP3, monthly Gumbel, and monthly LP3.

For Bayelsa, both the daily Gumbel and LP3 models exhibit generally close agreement with observed rainfall quantiles. Minor deviations occur in the intermediate

and upper quantiles, but neither model exhibits substantial departures across most of the daily rainfall distribution. This visual agreement is consistent with the relatively small Q-Q RMSE values reported in Table 9. The monthly rainfall diagnostics for Bayelsa reveal more pronounced differences between the two distributions. The Gumbel model exhibits systematic departures in the upper quantiles, where several observed rainfall maxima fall below their corresponding theoretical quantiles. This indicates that the fitted Gumbel model overestimates some upper-tail monthly rainfall quantiles within the plotted range. In contrast, the LP3 model demonstrates substantially closer alignment with the diagonal reference line across much of the distribution, supporting its lower Q-Q RMSE.

In Rivers State, the daily Gumbel and LP3 models exhibit close agreement across most observed rainfall quantiles. Minor deviations are visible in the upper tail, but both distributions reproduce the general pattern of annual maximum daily rainfall. The relatively small differences in Q-Q RMSE indicate broadly comparable fitting performance. For monthly rainfall in Rivers, the Gumbel model exhibits deviations in the middle and upper portions of the distribution. The LP3 model provides closer overall agreement with the observed quantiles, although some upper-tail departures remain. This pattern is consistent with the smaller Q-Q RMSE obtained for LP3.

In Delta State, the daily Gumbel model demonstrates close agreement with the observed rainfall quantiles, including much of the upper distribution. The LP3 model also provides a reasonable fit, but its deviations are somewhat greater, particularly among selected upper-tail observations. These findings support the lower Q-Q RMSE obtained for the Gumbel model. For monthly rainfall in Delta, the Gumbel model exhibits noticeable deviations in the upper quantiles, including several observations falling below the diagonal reference line. The LP3 model provides closer agreement across the observed distribution, particularly in the intermediate and upper quantile ranges.

Collectively, the Q-Q diagnostics indicate that both distributions provide reasonable representations of annual maximum daily rainfall, while LP3 generally produces closer agreement with annual maximum monthly rainfall observations. The results also reveal that upper-tail deviations differ among states and rainfall accumulation periods. These deviations are important because long-return-period estimates depend strongly on the fitted upper-tail behaviour.

3.6. Homogeneity Test of Rainfall Data

The results of the homogeneity analyses as presented in Table 10 indicate no statistically significant abrupt changes in annual rainfall totals across the three states at the 5% significance level. In Bayelsa State, the test identified 2011 as the candidate change-point year, with a test statistic of 126.00 and a *p*-value of 0.5189. Since the *p*-value exceeds the conventional significance threshold of 0.05, the null hypothesis of no abrupt change cannot be rejected. This finding indicates insufficient statistical evidence of a significant shift in the central tendency of annual rainfall totals in Bayelsa during the study period.

Similarly, Rivers State recorded a Pettitt test statistic of 128.00, with a candidate change-point year of 2011 and a *p*-value of 0.4970. The result is not statistically significant at the 5% level, indicating insufficient evidence of an abrupt change in annual rainfall totals. Although the test identified 2011 as a possible change-point location, the associated probability does not support interpreting this year as a statistically established rainfall-regime shift. In Delta State, the Pettitt test identified 2012 as the candidate change-point year, with a test statistic of 108.00 and a *p*-value of 0.7422. This relatively high *p*-value indicates insufficient evidence against the null hypothesis of no abrupt change. Consequently, the annual rainfall-total series for Delta does not exhibit a statistically significant change point under the applied Pettitt testing procedure.

The SNHT results provide an additional assessment of potential changes in the annual rainfall series. Bayelsa recorded an SNHT statistic of 3.9617, with a candidate split after 2011, while Rivers recorded a statistic of 4.1951, with a candidate split after 2012. Delta recorded an SNHT statistic of 3.2074, with a candidate split after 2012. The corresponding permutation-based *p*-values were 0.3375, 0.2950, and 0.4720 for Bayelsa, Rivers, and Delta, respectively.

All three SNHT permutation *p*-values exceed 0.05, indicating that none of the detected candidate changes is statistically significant under the applied permutation-testing framework.

The absence of statistically significant change points suggests that the applied tests did not detect strong evidence of abrupt changes in annual rainfall totals during 1983–2023.

Table 10. Annual rainfall-total Pettitt and SNHT diagnostics from the supplied CHIRPS data analysis (1983–2023).

State	Pettitt Year	Pettitt k	Pettitt_Approx_p	SNHT Split Year	SNHT_T	SNHT_Permutation_p	SNHT_p_Method
Bayelsa	2011	126	0.518897	2011	3.961681	0.3375	1999 random permutations, exchangeability assumed
Rivers	2011	128	0.496972	2012	4.195098	0.295	1999 random permutations, exchangeability assumed
Delta	2012	108	0.742227	2012	3.207373	0.472	1999 random permutations, exchangeability assumed

4. Discussion

The findings of this study provide insights into the spatial and temporal characteristics of rainfall variability and extremes across Bayelsa, Rivers, and Delta States in the Niger Delta, Nigeria, during 1983–2023. Using CHIRPS rainfall observations, the study evaluated annual rainfall variability, annual maximum daily and monthly rainfall, extreme-value distribution performance, threshold exceedances, return-period estimates, and potential changes in rainfall characteristics. The application of Bayesian Gumbel inference, classical Gumbel and Log-Pearson Type III (LP3) frequency analysis, Peaks-Over-Threshold (POT) modelling with the Generalized Pareto Distribution (GPD), and stationary and non-stationary Generalized Extreme Value (GEV) models provided complementary statistical perspectives on extreme-rainfall behaviour.

The discussion focuses on the geographical differences in rainfall characteristics, the sensitivity of extreme-rainfall estimates to probability distribution selection, the uncertainty associated with long-return-period extrapolation, and the implications of the findings for precipitation-hazard assessment and climate-resilient planning.

4.1. Rainfall Trends and Spatial Variability

The spatial variability observed in annual rainfall across Bayelsa, Rivers, and Delta States demonstrates the heterogeneous nature of precipitation characteristics within the Niger Delta. The analysis indicates that Bayelsa generally experiences the highest annual rainfall totals, followed by Rivers and Delta. These geographical differences are consistent with the influence of coastal proximity, atmospheric moisture transport, seasonal monsoon circulation, and local environmental conditions on rainfall distribution across southern Nigeria.

The statistically nonsignificant annual rainfall trends identified in the study suggest that the available evidence does not establish consistent monotonic changes in annual

precipitation totals during 1983–2023. However, the absence of statistical significance should not be interpreted as evidence that rainfall conditions remained unchanged. Substantial interannual variability was observed, indicating that annual precipitation fluctuated throughout the study period.

The cited studies describe that rainfall variability in Nigeria depends on geographical location, temporal aggregation, and regional atmospheric circulation patterns [45]. Earlier investigations also documented contrasting rainfall trends across observation stations in the Niger Delta [1]. Such differences highlight the importance of considering the spatial resolution of rainfall datasets, observational periods, and statistical methods when comparing precipitation trends.

A cited study using CHIRPS observations in the Volta River Basin reportedly identified statistically non-significant monotonic trends in annual rainfall despite variability in extreme-rainfall characteristics [46]. This comparison reinforces the distinction between changes in total annual precipitation and changes in rainfall extremes. Nevertheless, differences in geographical coverage, climatic conditions, and analytical procedures limit direct comparison between the two regions.

The present study also demonstrates the importance of distinguishing state-averaged rainfall totals from spatial rainfall distributions and annual maximum rainfall series. State-averaged annual totals summarize precipitation accumulation across large geographical areas, while annual maximum daily and monthly rainfall characterize the upper extremes of the corresponding rainfall distributions. These variables provide different information and should not be treated as interchangeable indicators of rainfall intensity or climate change.

The spatial differences observed across the three states have implications for regional precipitation-hazard assessment. Areas experiencing greater rainfall accumulation or higher estimated rainfall extremes warrant closer examination of drainage conditions, catchment response, land-use characteristics, and exposure to flooding. However, the geographical ordering of state-level rainfall statistics does not establish equivalent differences in flood risk because hydrological and socioeconomic conditions also influence flood occurrence and consequences.

The findings therefore support the use of geographically differentiated rainfall assessments rather than assuming uniform precipitation characteristics throughout the Niger Delta. They also emphasize the importance of evaluating annual totals and extreme-rainfall indicators separately when examining long-term rainfall variability.

4.2. Bayesian Gumbel Inference and Uncertainty in Extreme-Rainfall Estimation

Bayesian Gumbel inference provides a probabilistic framework for estimating extreme-rainfall characteristics while explicitly accounting for uncertainty in model parameters. Unlike classical point-estimation approaches, Bayesian inference represents the uncertainty associated with fitted parameters through posterior probability distributions. These distributions provide a basis for constructing credible intervals around rainfall return-level estimates.

The state-specific Bayesian analysis indicated geographical differences in the posterior location and scale parameters of annual maximum daily and monthly rainfall. For annual maximum daily rainfall, Bayelsa recorded posterior mean location and scale parameters of approximately 65.32 mm and 16.30 mm, respectively. Rivers recorded corresponding estimates of 61.63 mm and 13.69 mm, while Delta recorded 50.90 mm and 12.02 mm.

These estimates suggest that the fitted distribution of annual maximum daily rainfall is shifted toward higher magnitudes in Bayelsa compared with Rivers and Delta. The larger scale parameter in Bayelsa also indicates greater dispersion in its fitted annual daily

maxima distribution. However, posterior parameter differences alone do not establish statistically significant geographical contrasts without examining their joint uncertainty.

For annual maximum monthly rainfall, Bayelsa similarly recorded the highest posterior mean location and scale parameters, estimated at 522.24 mm and 88.27 mm, respectively. Rivers recorded corresponding values of 455.55 mm and 69.37 mm, while Delta recorded 420.45 mm and 60.10 mm.

The monthly parameter estimates demonstrate a similar geographical ordering to the daily results. Bayelsa exhibits the highest fitted location and scale parameters, followed by Rivers and Delta. This consistency suggests that geographical differences in the distributions of annual maximum rainfall are evident across both accumulation periods.

The posterior credible intervals provide additional information regarding the uncertainty of these parameter estimates. For annual maximum daily rainfall, the 95% highest-density intervals for the location parameter were approximately 60.02–70.54 mm in Bayelsa, 57.10–66.17 mm in Rivers, and 46.93–54.70 mm in Delta. The corresponding scale-parameter intervals were 12.42–20.41 mm, 10.45–17.31 mm, and 9.01–15.09 mm.

For annual maximum monthly rainfall, the posterior location-parameter intervals were approximately 492.46–549.64 mm in Bayelsa, 432.47–477.04 mm in Rivers, and 400.73–440.26 mm in Delta. The corresponding scale-parameter intervals were 68.61–110.45 mm, 53.80–86.26 mm, and 45.91–74.49 mm.

The widths of these intervals indicate uncertainty associated with the estimation of extreme-rainfall distribution parameters from the available 41-year observational record. This uncertainty becomes particularly important when fitted distributions are used to estimate rainfall magnitudes associated with recurrence intervals longer than the observational period.

Bayesian convergence diagnostics provide information on the numerical reliability of posterior sampling. The original analysis reports convergence diagnostics and posterior predictive plots for the six Bayesian fits. However, the complete numerical posterior summaries and sampler outputs were not available for independent reanalysis in the present verification. The reported convergence assessment should therefore be treated as provisional pending confirmation of R-hat, bulk and tail effective sample sizes, and divergent-transition counts for every chain. Even satisfactory convergence would not independently establish the suitability of the Gumbel distribution or the reliability of long-return-period extrapolation [47].

The interpretation of Bayesian return levels must also consider the distinction between parameter uncertainty and broader model uncertainty. Credible intervals quantify uncertainty conditional on the selected likelihood, prior distributions, and observed data. They do not automatically incorporate uncertainty arising from alternative probability distributions, possible non-stationarity, or systematic errors in the CHIRPS rainfall observations.

The cited Bayesian hydrology literature emphasizes the importance of representing parameter uncertainty when estimating rare environmental events [48,49]. The present findings support this approach by demonstrating geographical variation in posterior extreme-rainfall characteristics and the uncertainty associated with their estimation.

Bayesian Gumbel inference therefore provides a complementary basis for evaluating extreme-rainfall behaviour across the Niger Delta. Its principal contribution is the explicit characterization of parameter uncertainty, while its application to long-return-period rainfall estimation requires continued attention to model adequacy, posterior predictive performance, and the assumptions underlying the rainfall series.

4.3. Generalized Extreme Value Sensitivity Analysis

The Generalized Extreme Value (GEV) sensitivity analysis compared stationary and linearly time-varying-location models for annual maximum daily (AMAX-D) and annual maximum monthly (AMAX-M) rainfall in Bayelsa, Rivers, and Delta States. Each of the six series contained 41 annual maxima for 1983–2023. Both specifications were refitted using multiple optimizations starting values and parameter-support checks to reduce the risk of accepting an inferior numerical solution. The non-stationary specification permitted a linear temporal change in the location parameter, with scale and shape held constant over time.

The refitted stationary GEV models recorded lower Bayesian Information Criterion (BIC) values than their non-stationary counterparts for all six state–timescale comparisons. The Akaike Information Criterion (AIC) also favoured the stationary models in five comparisons. Delta monthly maxima constituted the exception: the non-stationary model recorded an AIC of 460.91 compared with 461.48 for the stationary model. This difference of approximately 0.58 provides little basis for selecting the more complex model.

For Delta monthly maxima, the corrected stationary fit yielded a log-likelihood of −227.74, AIC of 461.48, and BIC of 466.62. The corresponding non-stationary model yielded a log-likelihood of −226.45, AIC of 460.91, and BIC of 467.76. The likelihood-ratio statistic was 2.58, with an approximate chi-square p-value of 0.109 for one additional parameter. Therefore, the fitted temporal location component did not provide statistically significant improvement at the 5% level under this reference test. These values replace the earlier anomalous stationary solution with AIC near 613.93, which resulted from an inferior optimization outcome.

The non-stationary location slopes were approximately −0.125, +0.094, and +0.005 mm year^{-1} for daily maxima in Bayelsa, Rivers, and Delta, respectively. The corresponding monthly slopes were approximately −1.002, −0.908, and −1.410 mm year^{-1}. The six likelihood-ratio p-values were approximately 0.520, 0.394, 0.473, 0.333, 0.975, and 0.109 for Bayelsa daily, Bayelsa monthly, Rivers daily, Rivers monthly, Delta daily, and Delta monthly series, respectively. None reached the 5% significance threshold. These fitted slopes therefore should not be interpreted as statistically established trends in rainfall extremes.

Information criteria and likelihood-ratio results are conditional on the chosen model structures, observations, and optimization procedure. The likelihood-ratio p-values use a conventional asymptotic chi-square approximation, which warrants caution for samples containing only 41 annual maxima. Moreover, the failure to identify significant non-stationarity does not prove that rainfall extremes are strictly stationary or will remain so under future climate conditions. The outcome of the GEV sensitivity analysis presented in this study is consistent with previous studies that have emphasized the need for rigorous model comparison and uncertainty assessment when evaluating time-varying hydrological extremes [50–52].

The corrected evidence supports stationary GEV as a parsimonious reference model for the present record, with the linearly time-varying-location model retained as a sensitivity analysis. The fitted GEV comparisons do not provide statistically significant evidence of a linear temporal change in the location parameter for any of the six annual-maxima series.

4.4. Peaks-Over-Threshold and Generalized Pareto Distribution Analysis

The Peaks-Over-Threshold approach provides an alternative to annual block-maxima modelling by examining rainfall observations exceeding a specified high threshold. This method incorporates multiple extreme-rainfall events within individual

years and therefore provides additional information on the frequency and magnitude of high-rainfall occurrences.

The state-specific POT analysis revealed differences in the rainfall thresholds, temporal clustering, fitted GPD parameters, and return levels across Bayelsa, Rivers, and Delta States. At the selected 95th-percentile thresholds, Bayelsa recorded a rainfall threshold of 31.65 mm day^{-1}, compared with 27.43 mm day^{-1} in Rivers and 25.17 mm day^{-1} in Delta.

Each state recorded 749 raw exceedances at its respective empirical 95th-percentile threshold. The equal raw-exceedance counts arise from the percentile-based threshold definition and comparable observation counts rather than identical absolute rainfall exceedance frequencies.

Following the application of the three-day run-length declustering procedure, the number of retained extreme-rainfall events decreased to 470 in Bayelsa, 515 in Rivers, and 494 in Delta. These reductions correspond to approximately 37.2%, 31.2%, and 34.0% of the original exceedance counts, respectively.

The declustering results demonstrate the importance of accounting for temporal dependence in extreme-rainfall observations. Consecutive high-rainfall days frequently form part of the same meteorological event. Treating these observations as independent extremes would overstate the effective number of separate rainfall events and affect the estimated occurrence rates used in return-level calculations.

The fitted GPD shape parameters were approximately 0.0182 for Bayelsa, 0.0232 for Rivers, and −0.0194 for Delta. The corresponding scale parameters were 13.71 mm, 12.47 mm, and 10.84 mm.

The small positive shape estimates in Bayelsa and Rivers indicate fitted upper tails that are slightly heavier than the exponential limiting case, while the slightly negative estimate in Delta indicates a fitted upper tail with a finite endpoint under the assumed GPD model. However, the estimates are close to zero, and their uncertainty must be considered before drawing firm conclusions about differences in tail behaviour.

The threshold-sensitivity analysis further demonstrated that fitted GPD parameters depend on the selected exceedance threshold. Across the 90th to 99th percentiles, Rivers exhibited comparatively stable shape estimates, whereas Bayelsa and Delta showed more pronounced changes as the threshold increased.

These findings highlight the trade-off involved in selecting POT thresholds. Lower thresholds provide larger exceedance samples but risk including observations that do not adequately follow the asymptotic GPD approximation. Higher thresholds focus on more extreme observations but reduce the available sample size and increase parameter-estimation uncertainty.

The estimated 100-year POT-GPD daily rainfall return levels were approximately 134.70 mm in Bayelsa, 124.21 mm in Rivers, and 96.99 mm in Delta. These estimates indicate geographical differences in the fitted magnitudes of rare daily rainfall events, with Bayelsa recording the highest estimated return level.

The corresponding 50-year return levels were approximately 123.96 mm, 114.09 mm, and 90.40 mm for Bayelsa, Rivers, and Delta, respectively. The consistent geographical ordering suggests that Bayelsa exhibits the highest estimated upper-tail rainfall magnitudes under the fitted POT-GPD models.

The Q-Q and P-P diagnostics generally indicated reasonable agreement between the observed declustered excesses and fitted GPD distributions. However, deviations were evident in portions of the upper tails, emphasizing that satisfactory overall graphical agreement does not guarantee accurate estimation of the most extreme-rainfall quantiles.

The POT-GPD results are broadly comparable with the Gumbel-based daily return-level estimates, although differences arise from their distinct statistical sampling

frameworks. POT-GPD models threshold exceedances and their occurrence rates, whereas Gumbel block-maxima models use one annual maximum observation per year.

For example, the Gumbel-based 100-year daily rainfall return levels were approximately 136.71 mm in Bayelsa, 121.41 mm in Rivers, and 103.26 mm in Delta, compared with 134.70 mm, 124.21 mm, and 96.99 mm under POT-GPD. The differences indicate sensitivity to model formulation and event definition rather than necessarily demonstrating failure of either method which resonates with [50]

This approach can utilize more information from extreme precipitation events and is particularly relevant in regions where multiple intense rainfall episodes may occur within a year [53,54]. Its application to rainfall extremes has also been demonstrated in Nigeria by [55], who employed the Generalized Pareto Distribution (GPD) alongside block-maxima modelling to investigate extreme rainfall in Katsina. Similarly, a study conducted by [56] on extreme rainfall in Niamey, Niger, applied stationary and nonstationary POT-GPD models to assess rainfall thresholds and extreme-event characteristics emphasizing the importance of threshold selection, event independence, and uncertainty assessment. The present findings reinforce these considerations in the context of the Niger Delta which also corroborates [56].

The POT-GPD analysis therefore provides complementary evidence of geographical differences in extreme daily rainfall. Nevertheless, uncertainty associated with threshold selection, temporal dependence, upper-tail behaviour, and long-return-period extrapolation remains important when interpreting the resulting estimates.

4.5. Comparative Performance of the Gumbel and Log-Pearson Type III Distributions

The comparative analysis of the Gumbel and LP3 distributions demonstrate that model performance varies according to rainfall accumulation period, geographical location, and evaluation criterion. Both distributions were fitted to identical annual block-maxima samples within each state and rainfall accumulation period, ensuring that the comparisons were based on equivalent rainfall observations.

For annual maximum daily rainfall, the Gumbel distribution recorded lower AIC and BIC values than LP3 across all three states. In Bayelsa, the Gumbel model recorded an AIC of 357.63 and BIC of 361.06, compared with 359.63 and 364.77 for LP3. Similar patterns were observed in Rivers, where the corresponding values were 345.41 and 348.84 for Gumbel, compared with 346.58 and 351.72 for LP3.

In Delta, Gumbel recorded an AIC of 333.91 and BIC of 337.34, compared with 335.66 and 340.80 for LP3. These results indicate that the simpler Gumbel distribution provides a favourable balance between likelihood-based goodness of fit and model complexity for annual maximum daily rainfall across the three states.

However, the Q-Q diagnostics indicate that LP3 provides slightly closer empirical quantile agreement for daily rainfall in Bayelsa and Rivers. In Bayelsa, the Q-Q RMSE decreased from 3.20 mm under Gumbel to 3.12 mm under LP3, while the corresponding MAE decreased from 2.49 mm to 2.47 mm.

In Rivers State, LP3 reduced Q-Q RMSE from 2.18 mm to 2.00 mm and MAE from 1.64 mm to 1.45 mm. Conversely, Gumbel demonstrated better performance across all four evaluation criteria for annual maximum daily rainfall in Delta.

For annual maximum monthly rainfall, LP3 demonstrated closer empirical quantile agreement across all three states. In Bayelsa, the Q-Q RMSE decreased from 29.21 mm under Gumbel to 11.30 mm under LP3, while MAE decreased from 19.32 mm to 9.94 mm.

However, in River State, LP3 reduced Q-Q RMSE from 17.30 mm to 11.16 mm and MAE from 12.94 mm to 9.00 mm. Similarly, in Delta, Q-Q RMSE decreased from 15.02 mm to 7.31 mm, while MAE decreased from 11.28 mm to 6.26 mm.

The LP3 distribution also recorded lower AIC values for annual maximum monthly rainfall across all three states. Nevertheless, BIC favoured Gumbel in Rivers and Delta, indicating that the additional parameter flexibility of LP3 was not consistently supported after applying the stronger complexity penalty associated with BIC.

The results suggest that LP3 provides a closer representation of observed monthly rainfall quantiles, whereas Gumbel remains competitive when model complexity is considered. The small AIC and BIC differences in several comparisons indicate limited statistical separation between the competing distributions. The finding presented in this study resonates with [57,58] who highlighted the importance of distribution choice, record characteristics, and uncertainty in extreme-event frequency analysis. The results therefore support state-specific and accumulation-period-specific model evaluation, incorporating goodness-of-fit measures, information criteria, upper-tail diagnostics, and sensitivity analyses of design return levels.

The 100-year return-level estimates further demonstrate the influence of model selection. For annual maximum daily rainfall, the Gumbel estimates were approximately 136.71 mm in Bayelsa, 121.41 mm in Rivers, and 103.26 mm in Delta. The corresponding LP3 estimates reported in the comparison outputs were approximately 132.42 mm, 133.68 mm, and 108.23 mm.

These differences demonstrate that the geographical ordering of estimated rainfall extremes depends partly on the selected probability distribution. Although Bayelsa records the highest Gumbel-based daily return level, Rivers records a slightly higher estimate under LP3.

For annual maximum monthly rainfall, the Gumbel return levels were approximately 910.92 mm, 760.52 mm, and 684.28 mm for Bayelsa, Rivers, and Delta, respectively. The corresponding LP3 estimates reported in the comparison outputs were approximately 771.30 mm, 684.06 mm, and 613.34 mm.

The differences between the monthly Gumbel and LP3 estimates are substantial, particularly in Bayelsa. This demonstrates the sensitivity of long-return-period rainfall estimation to distributional assumptions and upper-tail behaviour.

However, lower AIC, BIC, or Q-Q errors do not establish that a model provides more accurate estimates of rainfall events beyond the observational record. The Q-Q RMSE and MAE values are descriptive in-sample diagnostics rather than independent out-of-sample predictive scores.

Similarly, high coefficients of determination obtained from descriptive regressions through model-generated return levels do not constitute independent evidence of probability-distribution adequacy. Such regressions summarize the shape of fitted return-level sequences but do not validate the underlying extreme-value model.

Previous studies describe geographical and methodological differences in the suitability of probability distributions for rainfall-frequency analysis in Nigeria [59–61]. The present findings support this broader observation by demonstrating that model preferences depend on rainfall accumulation period and the statistical criterion applied.

The results therefore support a state-specific and accumulation-period-specific approach to distribution selection rather than identifying one universally superior model. For practical flood-hazard assessment, model uncertainty should be evaluated alongside parameter uncertainty, particularly when estimating rainfall magnitudes associated with 50-year and 100-year recurrence intervals.

4.6. Homogeneity and Change-Point Analysis

The homogeneity analysis examined potential abrupt changes in annual rainfall totals across Bayelsa, Rivers, and Delta States during 1983–2023 using the Pettitt test and

Standard Normal Homogeneity Test (SNHT). These methods provide complementary assessments of possible changes in the central tendency of hydroclimatic time series.

The Pettitt test identified 2011 as the candidate change-point year for Bayelsa and Rivers, while 2012 was identified for Delta. The corresponding *p*-values were 0.5189, 0.4970, and 0.7422, respectively.

All three *p*-values exceed the 5% significance threshold, indicating insufficient statistical evidence to reject the null hypothesis of no abrupt change in annual rainfall totals. Consequently, the identified candidate years should not be interpreted as statistically confirmed rainfall-regime shifts.

The SNHT results provided a similar interpretation. Bayelsa recorded an SNHT statistic of approximately 3.96, with a candidate split after 2011 and a permutation *p*-value of 0.3375. Rivers recorded a statistic of approximately 4.20, with a candidate split after 2012 and a permutation *p*-value of 0.2950.

Delta recorded an SNHT statistic of approximately 3.21, with a candidate split after 2012 and a permutation *p*-value of 0.4720. None of these results was statistically significant at the 5% level.

The agreement between the Pettitt and SNHT significance assessments indicates that the available annual rainfall-total series do not provide statistically significant evidence of abrupt shifts in their central tendency during the study period.

Nevertheless, the absence of statistically significant change points does not establish strict homogeneity or stationarity. Statistical tests have limited power when changes are gradual, relatively small, or obscured by substantial interannual variability.

Furthermore, the homogeneity tests were applied to annual rainfall totals rather than annual maximum daily or monthly rainfall. The results therefore do not establish the presence or absence of statistically significant changes in the annual block-maxima series used for extreme-value frequency analysis.

This distinction is important because changes in rainfall extremes may occur independently of changes in annual precipitation totals. For example, an increase in the magnitude of extreme-rainfall events may coincide with little change in total annual precipitation if rainfall becomes concentrated into fewer high-intensity events.

Previous studies have highlighted the relevance of change-point analysis for identifying hydroclimatic variability in West Africa [43,44,62]. However, differences in geographical location, rainfall aggregation, and observational period limit direct comparison between reported change points across studies.

The use of satellite-derived rainfall observations also introduces considerations related to spatial representativeness, temporal consistency, and precipitation-estimation uncertainty. Previous evaluations of gridded precipitation products across West Africa have identified variations in rainfall-estimation accuracy among datasets, geographical locations, and aggregation periods [63,64]. Such limitations reinforce the need to interpret detected rainfall changes in relation to the characteristics of the underlying CHIRPS data rather than attributing statistical discontinuities directly to physical climate processes.

The present findings therefore support a cautious interpretation of rainfall homogeneity. Although no statistically significant abrupt changes were detected in annual rainfall totals, the results do not independently establish stationarity of the extreme-rainfall distributions. Additional state-specific trend and change-point analyses of annual maximum rainfall would provide stronger evidence regarding temporal changes in extreme precipitation.

4.7. Integrated Model Performance and Implications for Extreme-Rainfall Hazard Assessment

The combined findings highlight the importance of applying complementary statistical approaches to extreme-rainfall analysis rather than relying on a single

probability distribution or goodness-of-fit criterion. The Bayesian Gumbel model quantified parameter uncertainty, while classical Gumbel and Log-Pearson Type III (LP3) analyses demonstrated the sensitivity of rainfall return levels to distribution selection. The Peaks-Over-Threshold Generalized Pareto Distribution (POT-GPD) provided additional information on rainfall exceedances and upper-tail characteristics, whereas stationary and non-stationary Generalized Extreme Value (GEV) models assessed the influence of temporal assumptions. Recent studies emphasize the importance of integrating alternative extreme-value models and accounting for parameter uncertainty, model complexity, and distributional assumptions when estimating rare precipitation events [65].

The state-specific analyses revealed considerable geographical differences in estimated rainfall extremes, with Bayelsa generally recording the highest return levels under the Gumbel and POT-GPD models, followed by Rivers and Delta. However, the LP3 daily rainfall estimates demonstrated that geographical rankings could vary depending on the selected distribution. Similarly, Gumbel provided a more parsimonious representation of annual maximum daily rainfall according to AIC and BIC, whereas LP3 achieved closer empirical quantile agreement for annual maximum monthly rainfall. These findings indicate that model performance depends on rainfall accumulation period, geographical characteristics, and evaluation criteria. Consequently, closer agreement with observed quantiles does not necessarily guarantee more reliable extrapolation to rare rainfall events [66].

Stationary GEV models were preferred under BIC across all six rainfall series, with no significant improvement from the tested non-stationary formulations. However, this does not exclude future changes in rainfall extremes [67]. Overall, the study demonstrates the value of state-specific, multi-model rainfall-frequency analysis for precipitation-hazard assessment and infrastructure planning. Nevertheless, rainfall return levels should be integrated with hydrological and hydraulic modelling before application to flood-risk management, since rainfall extremes do not directly represent flood magnitudes or inundation probabilities [68].

5. Conclusions

This study examined rainfall variability and extreme precipitation characteristics across Bayelsa, Rivers, and Delta States in the Niger Delta, Nigeria, using CHIRPS rainfall observations from 1983 to 2023. By integrating Bayesian Gumbel inference, classical Gumbel and Log-Pearson Type III (LP3) distributions, Peaks-Over-Threshold Generalized Pareto Distribution (POT-GPD), stationary and non-stationary Generalized Extreme Value (GEV) models, and rainfall homogeneity tests, the study provides a comprehensive assessment of geographical differences, model performance, and uncertainty in extreme-rainfall estimation.

The main findings of the study are summarized as follows:

- Rainfall variability and trends: Bayelsa generally recorded the highest annual rainfall totals and extreme-rainfall magnitudes, followed by Rivers and Delta. However, annual rainfall trends were not statistically significant across the three states, indicating insufficient evidence of consistent monotonic changes during the study period.
- Gumbel return-level estimates: The estimated 100-year annual maximum daily rainfall return levels were 136.71 mm, 121.41 mm, and 103.26 mm for Bayelsa, Rivers, and Delta, respectively. The corresponding annual maximum monthly estimates were 910.92 mm, 760.52 mm, and 684.28 mm, demonstrating considerable geographical differences in extreme-rainfall magnitudes.

- Comparative model performance: Gumbel recorded lower AIC and BIC values for annual maximum daily rainfall across all three states, while LP3 generally provided closer empirical quantile agreement for annual maximum monthly rainfall. These differences highlight the influence of rainfall accumulation period, distribution selection, and evaluation criteria on model performance.
- Bayesian uncertainty assessment: Bayesian Gumbel analysis indicated higher posterior location and scale parameters in Bayelsa than in Rivers and Delta. However, the original posterior summaries and sampler diagnostics require independent verification before numerical convergence can be confirmed.
- POT-GPD extreme-rainfall estimates: The 95th-percentile daily rainfall thresholds were 31.65 mm, 27.43 mm, and 25.17 mm for Bayelsa, Rivers, and Delta, respectively. Following three-day declustering, 470, 515, and 494 extreme events were retained, producing 100-year daily rainfall return levels of 134.70 mm, 124.21 mm, and 96.99 mm, respectively.
- Stationarity and homogeneity assessment: Stationary GEV models were preferred under BIC across all six annual-maxima series, with no statistically significant improvement from the tested non-stationary formulations. Similarly, Pettitt and SNHT tests detected no significant abrupt changes in annual rainfall totals at the 5% significance level. Nevertheless, these results do not exclude possible future changes in rainfall extremes.

Overall, the study demonstrates that extreme-rainfall characteristics and model performance vary geographically and with rainfall accumulation period, emphasizing the importance of state-specific frequency analysis and uncertainty assessment. The findings provide useful information for preliminary rainfall-hazard screening, stormwater management, infrastructure planning, and climate adaptation across the Niger Delta. However, rainfall return levels should not be interpreted directly as flood magnitudes or inundation probabilities without supporting hydrological and hydraulic analyses.

Future research should integrate rainfall-frequency estimates with hydrological and hydraulic modelling, validate CHIRPS observations against available ground-based rainfall measurements, and investigate the effects of land-use change, antecedent soil moisture, and coastal processes on flood generation. Further assessment of non-stationary extreme-value models and alternative precipitation datasets would also improve confidence in long-return-period estimates.

Author Contributions: Conceptualization, O.I.; validation, A.R.L. and C.I.; formal analysis, O.I.; investigation, T.E.O.; resources, O.A.O.; data curation, O.A.O.; writing—original draft preparation, O.I.; writing—review and editing, A.R.L., C.I. and O.A.O.; visualization, C.I.; supervision, A.R.L. and C.I.; project administration, T.E.O.; funding acquisition, A.R.L. All authors have read and agreed to the published version of the manuscript.

Funding: This research received no extramural funding.

Data Availability Statement: The daily rainfall data used in this study for Bayelsa, Rivers, and Delta States, Nigeria, covering 1983–2023, were obtained from the Climate Hazards Group InfraRed Precipitation with Station Data (CHIRPS), developed by the Climate Hazards Center, University of California, Santa Barbara. The original CHIRPS dataset is publicly accessible at https://data.chc.ucsb.edu/products/CHIRPS/v2.0/ (accessed on 13 November 2026). The state-level rainfall series and supporting statistical analysis outputs are available from the corresponding author upon reasonable request.

Conflicts of Interest: The authors declare that there are no competing interests.

References

1. Mbachu, I.C. Probability distribution analysis of annual maximum precipitation in the Niger Delta: A critical step towards effective flood risk management. *J. Geogr. Environ. Earth Sci. Int.* **2024**, *28*, 95–109.
2. Notivoli, R.S.; -Salvador, A.M.; Lorenzo, R.G.; Sánchez, D.E.; García, C.C. Rainfall–runoff relationships at event scale in western Mediterranean ephemeral streams. *Hydrol. Earth Syst. Sci.* **2022**, *26*, 1243–1260. https://doi.org/10.5194/hess-26-1243-2022.
3. Ideki, O.; Weli, V.E. Analysis of rainfall variability using remote sensing and GIS in North Central Nigeria. *Atmos. Clim. Sci.* **2019**, *9*, 191–201.
4. Komi, S.K.; Kossi, K. Analysis of extreme rainfall in Oti River Basin (West Africa). *J. Water Clim. Chang.* **2021**, *12*, 1997–2009. https://doi.org/10.2166/wcc.2021.154.
5. Ideki, O.; Lupo, A.R. Analysis of Sea surface temperature pattern, variability and their teleconnection with rainfall dynamics over the Gulf of Guinea. *Springer J. Theor. Appl. Climatol.* **2024**, *155*, 8923–8950. https://doi.org/10.1007/s00704-024-05145-9.
6. Chukwu, S.; Otache, Y.; John, J.; Onemayin, D.; Ikugbiyi, S.; Yahaya, U.; Osoro, E. Characterization of rainfall pattern in northern Nigeria. *J. Res. For. Wildl. Environ.* **2024**, *15*, 30.
7. Yoshe, A.K. Sustainable Water Management Using Rainfall–Runoff Modelling in Rift Valley Basin, East Africa. *Adv. Environ. Eng. Res.* **2025**, *6*, 1–46. https://doi.org/10.21926/aeer.2501003.
8. Awode, A.E.; Adewumi, J.R.; Obiora-Okeke, O.; Komolafe, A.A. Analysis of rainfall variability and extreme events in South-Western Nigeria: Implications for water resource management and climate resilience. *Bull. Natl. Res. Cent.* **2025**, *49*, 31. https://doi.org/10.1186/s42269-025-01324-4.
9. Chukwudum, Q.C.; Gyamerah, S.A.; Nadarajah, S.; Hussam, E. Extreme rainfall transitions over West Africa. *Springer J. Stoch. Environ. Res. Risk Assess.* **2025**, *39*, 5789–5802. https://doi.org/10.1007/s00477-025-03086-x.
10. World Meteorological Organization (WMO). *Guidelines on the Definition and Characterization of Extreme Weather and Climate Events*; WMO-No. 1310; World Meteorological Organization: Geneva, Switzerland, 2023.
11. Gimeno, L.; Sorí, R.; Vázquez, M.; Stojanovic, M.; Algarra, I.; Eiras-Barca, J.; Gimeno-Sotelo, L.; Nieto, R. Extreme precipitation events. *WIREs Water* **2022**, *9*, e1611. https://doi.org/10.1002/wat2.1611.
12. Rodríguez-González, M.P.; Cerezo-Mota, R. Trend analysis of extreme precipitation indices and climate oscillations over the Yucatan Peninsula for the period 1980–2010. *Int. J. Climatol.* **2025**, *45*, e8885. https://doi.org/10.1002/joc.8885.
13. Wu, J. Extreme Rainfall Analysis and Return Period Estimation Based on Extreme Value Theory. *Eng. Proc.* **2026**, *128*, 31. https://doi.org/10.3390/engproc2026128031.
14. Yapo, A.L.M.; Yoroba, F.; Tiemoko, D.T.; Famien, A.M.L.; Touré, P.R.; Kouassi, B.K.; Kouadio, K.; Diawara, A. Assessment of precipitation and associated extremes in CORDEX simulations over Côte d'Ivoire. *Adv. Meteorol.* **2026**, *2026*, 9982320. https://doi.org/10.1155/adme/9982320.
15. Alam, M.A.; Emura, K.; Farnham, C.; Yuan, J. Best-fit probability distributions and return periods for maximum monthly rainfall in Bangladesh. *Climate* **2018**, *6*, 9. https://doi.org/10.3390/cli6010009.
16. Olanrewaju, R.; Ekiotuasinghan, B.; Akpan, G. Analysis of rainfall pattern and flood incidences in Warri metropolis, Nigeria. *Geogr. Environ. Sustain.* **2017**, *10*, 83–97. https://doi.org/10.24057/2071-9388-2017-10-4-83-97.
17. Deb, M.; Sun, N.; Yang, Z.; Wang, T.; Judi, D.; Cooper, M.G.; Wigmosta, M.S. Extreme flood return levels in a U.S. mid-Atlantic estuary using 40-year fluvial-coastal model simulations. *Sci. Data* **2025**, *12*, 1459. https://doi.org/10.1038/s41597-025-05566-9.
18. Eteh, D.R.; Japheth, B.R.; Chukwu-Okeah, G.; Nwosu, E.C.; Nwankwoala, H.O.; Eze, B.E.; Omietimi, E.J. Determination of flood hazard zones using GIS and remote sensing: A case study of Yenagoa Metropolis. *J. Geogr. Environ. Earth Sci. Int.* **2019**, *21*, 1–9. https://doi.org/10.9734/jgeesi/2019/v21i130116.
19. Echendu, A.J. The impact of flooding on Nigeria's Sustainable Development Goals (SDGs). *Ecosyst. Health Sustain.* **2020**, *6*, 1791735.
20. Olugonorisa, T.E.; Eludoyin, A.O.; Lateef, B. An Evaluation of Flood Fatalities in Nigeria. *Weather Clim. Soc.* **2022**, *14*, 709–720. https://doi.org/10.1175/wcas-d-21-0168.1.
21. Ogbozige, F.J. Development of intensity-duration-frequency (IDF) models for manually operated rain gauge catchment: A case study of Port Harcourt Metropolis using 50 years rainfall data. *Tanzan. J. Eng. Technol.* **2021**, *40*, 33–44. https://doi.org/10.52339/tjet.v40i2.731.
22. Najafi, M.S.; Kuchak, V.S. Ensemble-based monthly to seasonal precipitation forecasting for Iran using a regional weather model. *Int. J. Climatol.* **2024**, *44*, 4366–4387.

23. Ajibola, F.O.; Afolayan, S.A. Impacts of improved horizontal resolutions in the simulations of mean and extreme precipitation using CMIP6 High Res MIP models over West Africa. *Environ. Monit. Assess.* **2024**, *196*, 328. https://doi.org/10.1007/s10661-024-12492-7.
24. Ibe, C.C.; Dike, V.N.; Ishaya, S.K.; Magaji, J.I.; Ibe, A.A.; Anoruo, C.M. Projected near-future changes in precipitation extremes over Anambra-Imo River Basin inferred from CMIP6 HighResMIP. *Discov. Atmos.* **2024**, *2*, 8. https://doi.org/10.1007/s44292-024-00008-4.
25. Onyejuruwa, A.; Hu, Z.; Anosike, C.; Islam, A.R.M.T.; Madhushanka, D. Assessment of WRF model simulations of extreme rainfall events in West Africa: A comprehensive review. *Environ. Monit. Assess.* **2025**, *197*, 486. https://doi.org/10.1007/s10661-025-13932-8.
26. Oyegbile, O.; Chan, A.; Ooi, M.; Anwar, P.; Mohamed, A.A.; Li, L. Evaluation of WRF model performance with different microphysics schemes for extreme rainfall prediction in Lagos, Nigeria: Implications for urban flood risk management. *Bull. Atmos. Sci. Technol.* **2024**, *5*, 19. https://doi.org/10.1007/s42865-024-00081-y.
27. Abubakar, M.L.; Ahmed, M.S.; Ashiru, U.K.A.; Ahmed, M.; Mohammed, R.Z.; Abdussalam, A.F. Assessment of spatiotemporal rainfall variability over the Niger Delta region, Nigeria: Implications for water resource management. *Hydrol. Sci. J.* **2025**, *70*, 1571–1584. https://doi.org/10.1080/02626667.2025.2496279.
28. Agbonaye, A.I.; Izinyon, O.C. Rainfall Frequency Analysis of Some Cities in Niger Delta Region of Nigeria. *J. Appl. Sci. Environ. Manag.* **2024**, *28*, 659–664.
29. Agha, C.W.; Mokwenye, I.I.; Atikpo, E.; Nwulu, N. Gumbel Distribution-Based Flood Frequency Analysis for Coastal Flood Risk Assessment in Ugborodo Community, Niger Delta, Nigeria. *Environ. Technol. Sci. J.* **2025**, *16*, 133–143. https://doi.org/10.4314/etsj.v16i1.13.
30. Gobo, A.E.; Abam, T.K.S. Return period analysis as a tool for urban flood prediction in the Niger Delta: A case study of Port Harcourt City. *J. Environ. Hydrol.* **2006**, *14*, 1–10.
31. Ologunorisa, E.T. An Assessment of Flood Risk in the Niger Delta. Nigeria. Ph.D. Thesis, University of Port Harcourt, Port Harcourt, Nigeria, 2001, 303p.
32. Odekunle, T.O. The magnitude–frequency characteristic of rainfall in Ondo, Southwestern Nigeria. *Ife Res. Publ. Geogr.* **2001**, *8*, 36–41.
33. David, A.O.; Nwaogazie, I.L. Optimization technique in rainfall–intensity–duration–frequency modelling for Ikeja, South-West, Nigeria. *Niger. J. Technol.* **2021**, *39*, 1276–1285. https://doi.org/10.4314/njt.v39i4.37.
34. Abam, T.; Nwankwoala, H. Hydrogeology of Eastern Niger Delta: A review. *J. Water Resour. Prot.* **2020**, *12*, 741–777. https://doi.org/10.4236/jwarp.2020.129045.
35. Nwankwoala, H.; Okujagu, D.C. A review of wetlands and coastal resources of the Niger Delta: Potentials, challenges, and prospects. *Environ. Ecosyst. Sci.* **2021**, *5*, 37–46.
36. Crétat, J.; Harrison, S.P.; Braconnot, P.; d'Agostino, R.; Jungclaus, J.; Lohmann, G.; Shi, X.; Marti, O. Orbitally forced and internal changes in West African rainfall interannual-to-decadal variability for the last 6000 years. *Clim. Dyn.* **2024**, *62*, 2301–2316.
37. Nigeria Governors Forum. Public Finance Database. 51, Lake Chad Crescent Maitama, Abuja Federal Capital Territory, Nigeria. 2026. Available online: www.ngf.org.ng (accessed on 15 November 2026).
38. Agumagu, O.O.; Marchant, R.; Stringer, L.C. Land use and land cover change dynamics in the Niger Delta region of Nigeria from 1986 to 2024. *Land* **2025**, *14*, 765. https://doi.org/10.3390/land14040765.
39. Dike, E.C.; Amaechi, C.V.; Beddu, S.B.; Weje, I.I.; Ameme, B.G.; Efeovbokhan, O.; Oyetunji, A.K. Coastal vulnerability index sensitivity to shoreline position and coastal elevation parameters in the Niger Delta region, Nigeria. *Sci. Total Environ.* **2024**, *919*, 170830. https://doi.org/10.1016/j.scitotenv.2024.170830.
40. Bisong, A.E.; Miepamo, W.; Ndinyenma, W.P.; Douye, W.P.E. Assessment of flood vulnerability levels in the Lower Orashi River, Niger Delta region, Nigeria. *J. Geogr. Environ. Earth Sci. Int.* **2024**, *28*, 87–106. https://doi.org/10.9734/jgeesi/2024/v28i5772.
41. Funk, C.; Peterson, P.; Landsfeld, M.; Pedreros, D.; Verdin, J.; Shukla, S.; Husak, G.; Rowland, J.; Harrison, L.; Hoell, A.; et al. The climate hazards infrared precipitation with stations—A new environmental record for monitoring extremes. *Sci. Data* **2015**, *2*, 150066. https://doi.org/10.1038/sdata.2015.66.
42. Gumbel, E.J. The return period of flood flows. *Ann. Math. Stat.* **1941**, *12*, 163–190.
43. Alexandersson, H. A homogeneity test applied to precipitation data. *J. Climatol.* **1986**, *6*, 661–675. https://doi.org/10.1002/joc.3370060607.
44. Pettitt, A.N. A non-parametric approach to the change-point problem. *Appl. Stat.* **1979**, *28*, 126–135.

45. Ibebuchi, C.C.; Abu, I.O. Rainfall variability patterns in Nigeria during the rainy season. *Sci. Rep.* **2023**, *13*, 7888. https://doi.org/10.1038/s41598-023-34970-7.
46. Akanbi, O.B. Bayesian Modeling of Extreme Rainfall Data of Some Selected Locations in Nigeria. *J. Sci. Res. Rep.* **2020**, *26*, 16–26. https://doi.org/10.9734/jsrr/2020/v26i130209.
47. Vehtari, A.; Gelman, A.; Simpson, D.; Carpenter, B.; Bürkner, P.-C. Rank-normalization, folding, and localization: An improved (\hat{R}) for assessing convergence of MCMC. *Bayesian Anal.* **2021**, *16*, 667–718.
48. Tian, D.; Wang, L. BLP3-SP: A Bayesian Log-Pearson Type III Model with Spatial Priors for Reducing Uncertainty in Flood Frequency Analyses. *Water* **2022**, *14*, 909. https://doi.org/10.3390/w14060909.
49. Zorzetto, E.; Canale, A.; Marani, M. A Bayesian non-asymptotic extreme value model for daily rainfall data. *J. Hydrol.* **2024**, *628*, 130378.
50. Katz, R.W.; Parlange, M.B.; Naveau, P. Statistics of extremes in hydrology. *Adv. Water Resour.* **2002**, *25*, 1287–1304. https://doi.org/10.1016/S0309-1708(02)00056-8.
51. Slater, L.J.; Anderson, B.; Buechel, M.; Dadson, S.; Han, S.; Harrigan, S.; Kelder, T.; Kowal, K.; Lees, T.; Matthews, T.; et al. Nonstationary weather and water extremes: A review of methods for their detection, attribution, and management. *Hydrol. Earth Syst. Sci.* **2021**, *25*, 3897–3935. https://doi.org/10.5194/hess-25-3897-2021.
52. Bossa, A.Y.; Akpaca, J.d.D.; Hounkpè, J.; Yira, Y.; Badou, D.F. Non-stationary flood discharge frequency analysis in West Africa. *GeoHazards* **2023**, *4*, 316–327. https://doi.org/10.3390/geohazards4030018.
53. Coles, S. *An Introduction to Statistical Modeling of Extreme Values*; Springer: Berlin/Heidelberg, Germany, 2001. https://doi.org/10.1007/978-1-4471-3675-0.
54. Solari, S.; Losada, M.A. A unified statistical model for hydrological variables including the selection of threshold for the peak over threshold method. *Water Resour. Res.* **2012**, *48*, W10541. https://doi.org/10.1029/2011WR011475.
55. Kane, I.L.; Tahir, K.U.; Rabe, A. Extreme rainfall modeling through the lens of extreme value theory: A case study of Katsina City, Nigeria. *UMYU Sci.* **2023**, *2*, 92–99. https://doi.org/10.56919/usci.2323.015.
56. Garba, I.; Abdourahamane, Z.S. Extreme rainfall characterisation under climate change and rapid population growth in the city of Niamey, Niger. *Heliyon* **2023**, *9*, e13326. https://doi.org/10.1016/j.heliyon.2023.e13326.
57. Scarrott, C.; MacDonald, A. A review of extreme value threshold estimation and uncertainty quantification. *REVSTAT—Stat. J.* **2012**, *10*, 33–60. https://doi.org/10.57805/revstat.v10i1.110.
58. Serinaldi, F.; Kilsby, C.G. Rainfall extremes: Toward reconciliation after the battle of distributions. *Water Resour. Res.* **2014**, *50*, 336–352. https://doi.org/10.1002/2013WR014211.
59. Nwaogazie, I.L.; Sam, M.G.; David, A.O. Predictive performance analysis of PDF–IDF model types using rainfall observations from fourteen gauged stations. *Int. J. Environ. Clim. Change* **2021**, *11*, 125–143. https://doi.org/10.9734/ijecc/2021/v11i130349.
60. Emeka-Chris, C.C. Generation of rainfall intensity-duration frequency models for Port Harcourt City in South-South Nigeria. *Arid. Zone J. Eng. Technol. Environ.* **2024**, *20*, 403–416.
61. Okagbare, O.A.; Izinyon, O.C.; Agbonaye, A.I. Best fit probability distribution/parameter estimation procedure for precipitation frequency analysis at some stations in Southern Nigeria. *NIPES J. Energy Technol. Environ.* **2024**, *6*, 58–70. https://doi.org/10.5281/zenodo.14523597.
62. Ekwezuo, C.S.; Ezeh, C.U.; Sogbedji, J.M.; Phil-Eze, P.O. Analysing spatial variability of monsoon rainfall over West Africa. *Int. J. Environ. Clim. Change* **2024**, *14*, 77–91. https://doi.org/10.9734/ijecc/2024/v14i94394.
63. Satgé, F.; Defrance, D.; Sultan, B.; Bonnet, M.-P.; Seyler, F.; Rouché, N.; Pierron, F.; Paturel, J.-E. Evaluation of 23 gridded precipitation datasets across West Africa. *J. Hydrol.* **2020**, *581*, 124412. https://doi.org/10.1016/j.jhydrol.2019.124412.
64. Kouakou, C.; Paturel, J.-E.; Satgé, F.; Tramblay, Y.; Defrance, D.; Rouché, N. Comparison of gridded precipitation estimates for regional hydrological modeling in West and Central Africa. *J. Hydrol. Reg. Stud.* **2023**, *47*, 101409. https://doi.org/10.1016/j.ejrh.2023.101409.
65. Macharia, D.; Fankhauser, K.; Selker, J.S.; Neff, J.C.; Thomas, E.A. Validation and Intercomparison of Satellite-Based Rainfall Products over Africa with TAHMO In Situ Rainfall Observations. *J. Hydrometeor.* **2022**, *23*, 1131–1154. https://doi.org/10.1175/JHM-D-21-0161.1.
66. Jayaweera, L.; Wasko, C.; Nathan, R. Evidence for non-stationarity in the GEV shape parameter when modeling extreme rainfall. *Water Resour. Res.* **2025**, *61*, e2023WR036426. https://doi.org/10.1029/2023WR036426.

67. Rischmuller, A.L.; Poschlod, B.; Sillmann, J. Bayesian hierarchical modelling of intensity-duration-frequency curves using a climate model large ensemble. *Adv. Stat. Climatol. Meteorol. Oceanogr.* **2026**, *12*, 1–19. https://doi.org/10.5194/ascmo-12-1-2026.
68. Markus, M.; Wu, S.; Wang, F.; Lorenz, D.; Koric, S.; Grady, K.; Angel, J. Design and evaluation of methodology for nonstationary precipitation frequency analysis in the Northeastern United States. *Front. Earth Sci.* **2026**, *20*, 1–11. https://doi.org/10.1007/s11707-025-1196-4.

Disclaimer/Publisher's Note: The statements, opinions and data contained in all publications are solely those of the individual author(s) and contributor(s) and not of MDPI and/or the editor(s). MDPI and/or the editor(s) disclaim responsibility for any injury to people or property resulting from any ideas, methods, instructions or products referred to in the content.